Eclogite Facies Regional Metamorphism of Hydrous Mafic Rocks in the Central Alpine Adula Nappe

by CHRISTOPH A. HEINRICH*

Departement für Erdwissenschaften, Eidgenössische Technische Hochschule, Zürich, CH-8092, Switzerland

(Received 9 November 1984; revised typescript accepted 19 June 1985)

ABSTRACT

The Adula Nappe is a slice of Pre-Mesozoic continental basement affected by Early Alpine (Mesozoic or Lower Tertiary) high-pressure metamorphism. Mineral compositions in mafic rocks containing omphacite + garnet + quartz record a continuous regional trend of increasing recrystallization temperatures and pressures that can be ascribed to this regional high-pressure metamorphic event. *P-T* estimates derived from mineral compositions grade from about 12 kb and 500 °C or less in the north of the nappe to more than 20 kb/800 °C in the south.

The regional *P-T* trend is associated with a mineralogical transition from assemblages containing additional albite and abundant amphiboles, epidote minerals, and white micas in the north (omphacite-garnet amphibolites) to kyanite eclogites containing smaller amounts of hornblende and zoisite in the south. Textures and mineral compositional data show that these hydrous and anhydrous silicates associated with omphacite + garnet + quartz are primary parts of the high-pressure assemblages. Observed phase relations between these primary silicates, theoretical Schreinemakers analysis, and the thermobarometric results, together indicate that the regional transition from omphacite amphibolites to kyanite eclogites can be described by two simplified reactions:

$$\text{alb} + \text{epi} + \text{hbl} = \text{omp} + \text{kya} + \text{qtz} + \text{par} \quad (\text{H}_2\text{O-conserving}) \qquad (15)$$

$$\text{par} + \text{epi} + \text{hbl} + \text{qtz} = \text{omp} + \text{kya} + \text{H}_2\text{O} \quad (\text{dehydration}) \qquad (12)$$

which have the character of isograd reactions.

Local variations of water activity (a_{H_2O}) as indicated by isofacial mineral assemblages, and the H_2O-conserving character of the reaction (15), are interpreted to reflect largely H_2O-undersaturated and predominantly *fluid-absent* high-pressure metamorphism within the northern part of the nappe. The omphacite amphibolites and paragonite eclogites in this area are thought to have formed by H_2O-conserving reactions from Pre-Mesozoic high-grade amphibolites, i.e. from protoliths of similar bulk H_2O-content.

The second 'isograd' (12) is interpreted to mark the regional transition from largely *fluid-absent* metamorphism in the north to fluid-present metamorphism in the south, where metamorphic pressures and temperatures in excess of 12–15 kb and 500–600 °C were sufficient for prograde *in-situ* dehydration of similar hydrous protoliths to kyanite eclogites. The observation of abundant veins, filled with quartz + kyanite + omphacite, suggests that a free fluid coexisted locally with the kyanite eclogites of the southern Adula Nappe at some time during progressive dehydration.

INTRODUCTION

Dehydration of hydrous mafic rocks and associated metasediments to eclogitic rocks during subduction of oceanic crust is believed to be an important factor in the formation of partial melts in the descending slab, the overlying mantle, or the lower crust, giving rise to

* Present address: Bureau of Mineral Resources, Geology and Geophysics, Division of Petrology and Geochemistry, GPO Box 378, Canberra, ACT 2601, Australia.

calc-alkaline orogenic magmatism (e.g. Green & Ringwood, 1968; Wyllie, 1971, p. 208). Evidence for high-pressure dehydration of mafic rocks to eclogites has been established by experiments concentrating mainly on dehydration-melting relationships at relatively high temperatures (e.g. Lambert & Wyllie, 1972). However, little is yet known about which subsolidus mineral reactions are important under the lower-temperature conditions likely to prevail in the thermally disturbed realm of a subduction or continental collision zone (Anderson *et al.*, 1978; England & Thompson, 1984; Rubie, 1984).

Eclogites currently found in crustal metamorphic terrains often contain assemblages indicating high pressures and low to moderate temperatures, and many authors have therefore interpreted eclogite occurrences as evidence for earlier crustal subduction (e.g. Krogh, 1977; Evans & Trommsdorff, 1978; Evans *et al.*, 1979; Ernst & Dal Piaz, 1978; Rubie, 1984). However, it is not clear whether any of these 'crustal' eclogites have indeed formed by dehydration of more hydrous mafic precursors, or whether they have crystallized under H_2O-undersaturated conditions from primarily anhydrous protoliths. The latter possibility was first suggested by Bearth (1959) for nearly anhydrous eclogitic pillow metabasalts embedded in glaucophane-rich metahyaloclastites in the Western Alps. The concept that eclogites found in metamorphic terrains represent the H_2O-undersaturated equivalents of blueschist or amphibolite assemblages, forming at the same P-T conditions but higher H_2O activity, has been supported more generally by Fry & Fyfe (1969), Newton & Fyfe (1976) and in many textbooks (e.g. Miyashiro, 1973, p. 318; Winkler, 1974, p. 274). Other authors have stressed the observation of eclogitic veins and primary hydrous silicates as evidence for the presence of a fluid and high H_2O activity during the formation of some eclogites (Essene & Fyfe, 1967; Holland, 1979*a*; Brown & Bradshaw, 1979).

Eclogites from various terrains are mineralogically diverse (Smulikowski, 1964; Coleman *et al.*, 1965) and have probably formed under a wide range of P-T-a_{H_2O} conditions. However, comparison between eclogites and a more general interpretation of their genesis is hampered by the structural incoherence typical of most terrains, which rarely show regular regional distribution patterns of eclogitic assemblages. The few known exceptions are from SW Norway (Krogh, 1977; Griffin *et al.*, 1984), New Caledonia (Black, 1977), the Adula Nappe (Heinrich, 1982), and from Venezuela, where Maresch (1983) first reported a field example indicating progressive *in-situ* dehydration of amphibolite to eclogite. Recently, Takasu (1984) presented textural evidence for the transformation of epidote amphibolite to hydrous eclogite, which he ascribed to prograde dehydration metamorphism.

The Central Alpine Adula Nappe (Switzerland) displays a regionally systematic sequence of high-pressure assemblage in mafic rocks, grading from hydrosilicate-rich garnet + omphacite + quartz-bearing amphibolites, blueschists and eclogites in the north, to quartz-kyanite eclogites containing only minor hornblende and zoisite in the south (Heinrich, 1982, 1983). The southernmost occurrences are associated with garnet metaperidotites (Ernst, 1977, 1978; Evans & Trommsdorff, 1978; Evans *et al.*, 1979). This suite of hydrous mafic rocks has been chosen for a petrological study, to define some of the mineral reactions that are likely to control the formation of different omphacite + garnet + quartz-bearing assemblages, and to place some constraints on the conditions under which hydrous mafic protoliths may undergo prograde dehydration to hydrate-poor eclogites.

REGIONAL GEOLOGY AND STRUCTURAL RELATIONS

Structure and lithology of Adula Nappe

The Adula Nappe is an east- to southward dipping sheet-like body with an estimated thickness of 2–4 km, continuously exposed along a north–south profile of 50 km. It consists

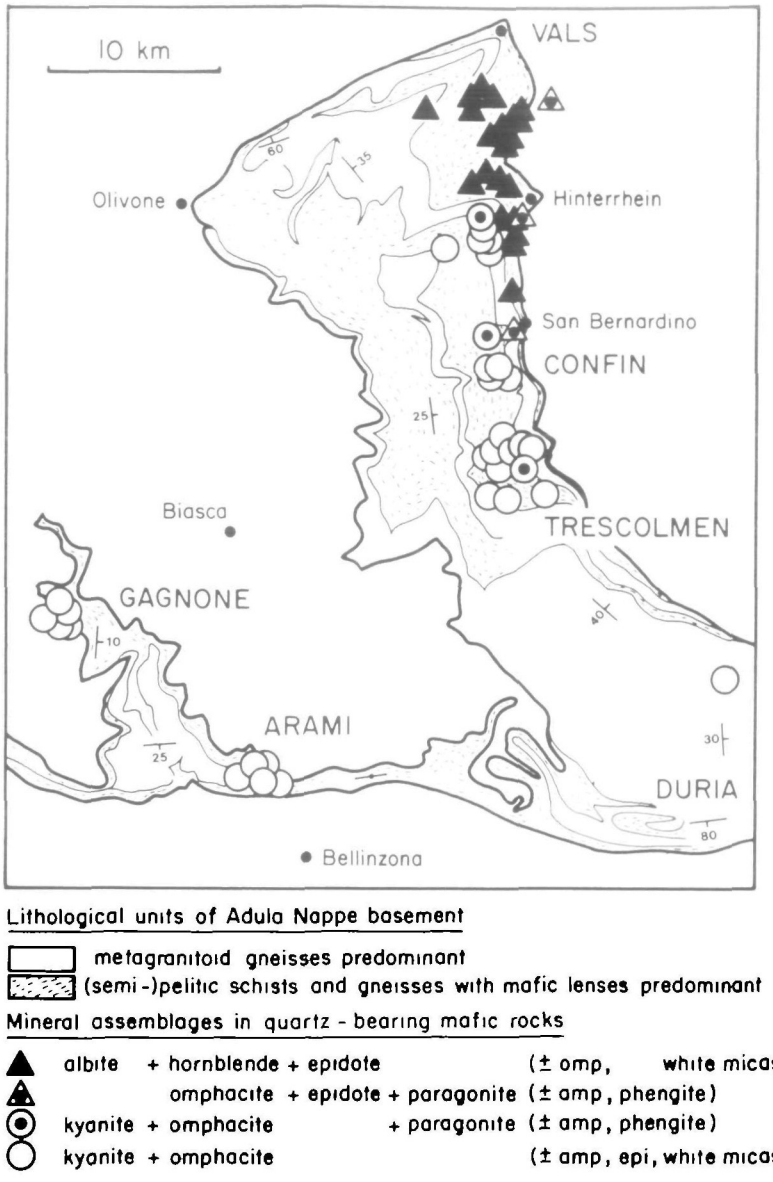

FIG. 1. Geological map showing the outline and internal structure of the Adula Nappe in southern Switzerland (simplified from Heinrich, 1983, plate 1). The metasedimentary units of the Adula Nappe host mafic lenses containing high-pressure assemblages. Occurrences of diagnostic quartz-bearing assemblages are indicated by specific symbols, including some data by Baumgartner (1981).

predominantly of metagranitic and metapelitic gneisses and schists of a Pre-Mesozoic continental basement, which has been affected first by Mesozoic or lower Tertiary high-pressure metamorphism, followed by Oligocene Barrovian-style metamorphism. The two main rock types are interlayered on a kilometre scale grossly parallel to the nappe structure (Fig. 1). High-pressure assemblages are mainly preserved in mafic lenses within the metasedimentary layers (Heinrich, 1982; including additional references).

Carboniferous Rb/Sr age data indicating an event of Pre-Alpine high-grade metamorphism are preserved in some white micas from the northern Adula Nappe (Frey *et al.*, 1976). Rb/Sr whole rock data suggest a Variscan (Late Carboniferous) origin for migmatites in the southern Adula Nappe, with local remobilization during Tertiary amphibolite facies metamorphism (Hänny *et al.*, 1975). Some mafic high-pressure assemblages in the northern part of the nappe can be shown to derive from earlier high-grade amphibolites on the basis of locally preserved relict textures, in which glaucophane rims and sphene precipitates have partly replaced coarse-grained, formerly Ti-rich hornblendes with an earlier parallel alignment (Plas, 1959, p. 526; Heinrich, 1983, p. 78). Since the metasedimentary layers enclosing the mafic rocks extend over most of the length of the nappe, a similar amphibolitic origin is likely for the majority of the eclogitic rocks described in this paper. As in mafic rocks from other units of Variscan continental basement in the Alps, which are less affected by Alpine metamorphism (e.g. Buletti, 1983), trace element geochemistry indicates an ultimate origin from oceanic basalts for at least some of the Adula (Evans *et al.*, 1979, 1981; Aurisicchio *et al.*, 1982).

Mesozoic carbonate-rich to pelitic metasediments and minor metabasites separate the Adula Nappe from over- and underlying basement nappes. Some of this material has been imbricated at least into the frontal (northern) part of the Adula Nappe prior to all recognized stages of Alpine metamorphism and deformation (Jenny *et al.*, 1923; Plas, 1959; Egli, 1966; Baumgartner & Löw, 1983). Nevertheless, Mesozoic rocks comprise at most a few volume per cent of the present Adula Nappe.

The time of eclogite facies metamorphism has not been dated radiometrically, but geological evidence constrains it to the interval between Late Jurassic and Early Tertiary (Heinrich, 1982; 1983, p. 175).

Post-eclogite facies deformation and overprinting

Rocks containing garnet + omphacite + quartz (referred to as eclogitic assemblages sensu lato) are distributed over most of the Adula Nappe. They usually occur as relicts in cores of mafic lenses, where they escaped later deformation and hydration to lower-pressure greenschist and amphibolite assemblages. Heinrich (1982) described some key exposures which show that eclogite facies metamorphism was shared by the (semi-)pelitic country rocks. In most places, however, high-pressure assemblages were preserved in mafic rocks only. The phengite- and paragonite-rich high-pressure assemblages of the pelitic rocks were usually completely overprinted by prograde, biotite + feldspar-forming dehydration reactions, which occurred during later amphibolite facies metamorphism (Heinrich, 1982).

Post-eclogite deformation of schists and gneisses included isoclinal folding which reaches the scale of kilometres in the southern part of the nappe (Jenny *et al.*, 1923; Egli, 1966; Codoni, 1981). This deformation probably occurred before and during nappe emplacement and Oligocene Barrovian-type metamorphism, but after regional eclogite facies metamorphism. No original length scale can therefore be attributed to the still regular, but certainly distorted and blurred, exposed distribution pattern of eclogitic assemblages.

PETROGRAPHY OF ECLOGITIC ASSEMBLAGES

Mineral textures in thin section, combined with structural observations in zoned mafic lenses, allow a clear distinction of assemblages produced by post-eclogite overprinting from earlier eclogite facies assemblages. Overprinting to amphibolite or greenschist invariably proceeded via a texturally distinctive intermediate stage, involving symplectite pseudo-

TABLE 1

Primary assemblages and visually estimated modal composition of rocks studied by electron microprobe

	gar	*cpx*	*kya*	*qtz*	*amp*	*zoi*	*clz–epi*	*par*	*phe*	*additional phases*
Vals										
Ad42-9-14*	15	15		5	20 hbl		10		15	20 alb; pyr; rut
VA30	20	20		x	40 hbl		x		x	pyr; rut; clc
Ad41-9-20	5	20		10	5 hbl	15		5	5	pyr; sph; gra
Ad65-0-8*	10	5		x	60 glc		10		5	pyr; sph
Confin										
Ad48-9-5*	35	30		5	15 hbl			5	x	pyr; rut
E5-10	20	30	5	10	20 bar			5	10	pyr; rut
E5-6	35	35		10	5 hbl		10			rut
Ad51-9-12	10	45		x	15 hbl	25	5			pyr; rut; sph
Ad51-9-17		20		x	20 act	15				50 dol; clc; pyr; sph
Trescolmen										
Ad25-9-3*	30	40	10	x	10 hbl	x			5	rut
Ad61-9-1*	20	15	10	30	15 glc			5		5 tlc; pyr; rut
Gagnone										
CH271*	35	35	10	10	10 hbl					rut; ilm
Mg163K	35	35		15	10 hbl	x				rut; ilm
Mg163-4-8	35	35		20	20 hbl	20				rut
E2-2	20	30		x	30 hbl	5	10			rut
Arami										
Mg9-5-12c*	40	45	5	x	5 hbl	5				rut; ilm

Numbers refer to volume per cent, x = 2–5 per cent. * denotes samples for which silicate analyses are given in Tables 2 and 3 Exact sampling localities and some petrographic observations are listed in Appendix 1.

The following abbreviations for mineral phases are used throughout: act = actinolite, alb = albite, amp = amphibole, bar = barroisite, clc = calcite, clz = clinozoisite, cpx = clinopyroxene, dol = dolomite, epi = epidote, gar = garnet, glc = glaucophane, gra = graphite, hbl = hornblende, ilm = ilmenite, jad = jadeite, kya = kyanite, mus = muscovite, omp = omphacite, par = paragonite, phe = phengite, pyr = pyroxene, plg = plagioclase, qtz = quartz, rut = rutile, sph = sphene, tlc = talc, zoi = zoisite.

morphs and thin reaction rims along grain boundaries (Heinrich, 1982). By contrast, the minerals here considered to be part of a '*primary eclogitic assemblage*', which are the subject of this study, are characterized texturally by sharp mutual grain boundaries, and by grains comparable or larger in size than omphacite and quartz (Table 1, Appendix 1, Fig. 2). Many of the assemblages so defined show equigranular textures with or without a linear or planar parallel orientation shared by a variety of anhydrous and hydrous silicates. Some minerals can occur as euhedral (garnet) or anhedral-poikilitic (hornblende, kyanite, primary albite) porphyroblasts. Amphibole poikiloblasts appear to overgrow the aligned fabric in the matrix of some eclogites, but mutual inclusions involving minerals of similar composition, such as hornblende + garnet + omphacite + quartz inclusions in kyanite next to kyanite + garnet + omphacite + quartz inclusions in hornblende (e.g. CH271, Ad25-9-3), indicate a largely contemporaneous crystallization of hydrous and anhydrous 'primary' silicates. Even the highest-grade kyanite eclogites (see below) from the Arami eclogite-garnet meta-peridotite complex contain zoisite and hornblende in parallel alignment with equigranular garnet + omphacite + kyanite + quartz, and homogeneous garnet grains contain inclusions of hornblende of the same composition as the matrix. Despite extensive overprinting by texturally later and chemically different amphibole assemblages, there is little evidence to suggest (cf. Ernst, 1977, p. 377) that *all* hydrous phases formed at the expense of an earlier, completely anhydrous eclogite assemblage.

In the porphyroblastic eclogite textures, chemical equilibrium was probably approached at least at contacting grain boundaries, but rarely attained throughout a whole rock even at

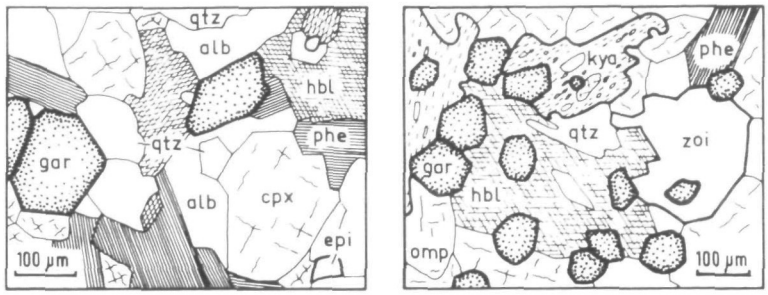

FIG. 2. Typical mineral textures of primary high-pressure assemblages. (left) Amphibolite Ad42-9-14 from Vals, with coexisting omphacite + albite + quartz + garnet + hydrous silicates. (right) Quartz-kyanite eclogite Ad25-9-3 from Trescolmen, with primary hornblende, zoisite and phengite. See Table 1 for mineral abbreviations.

the scale of a thin section. This is shown by the chemical zoning of larger mineral grains, indicated by arrows in Figs. 3, 8, 9 and 10, and discussed below. Deviation from complete equilibration is particularly obvious in chemically and texturally zoned garnet porphyroblasts, which in their Fe- and Ca-enriched core contain inclusions of biotite, sphene and rarely plagioclase (phases that do not occur in the eclogite matrix) and of dark green amphibole, which has a highly aluminous composition different from the pale bluish to brown matrix amphiboles. These inclusions could represent armoured relics of Pre-Alpine amphibolite assemblages, but the presence of omphacite and epidote as additional inclusion minerals indicates that the inclusion assemblages probably record an early (omphacite-epidote amphibolite?) stage in the Alpine high-pressure metamorphic history of eclogite formation (see below).

Many kyanite eclogites, especially in the Trescolmen area (Fig. 1), contain irregular veins 10–100 mm in width and less than a metre in length. The veins are filled with quartz, minor omphacite, sometimes apatite, and euhedral kyanite crystals up to several centimetres in size. In many cases they cut eclogite schistosity and banding. Vein walls show no obvious mineralogical zonation or alteration of the adjacent host eclogite. All matrix minerals of the host eclogite occur at the vein contact, with omphacite sometimes growing as needles into the vein. Although quartz has recrystallized to polygonal grains, the textural relations indicate that all vein minerals crystallized from a vein fluid which was probably in local equilibrium with the immediately adjacent kyanite eclogite.

Quartz and kyanite contain fluid inclusions up to 20 μm in size. Most inclusions are H_2O-rich with a small gas bubble, but highly saline inclusions with cubic ?NaCl daughter crystals have also been observed. No microthermometric studies have been performed so far, because most fluid inclusions are clearly secondary. At least the high-salinity inclusions have probably formed during amphibolite facies overprinting. This is indicated by their arrangement along healed fractures in the extension of hairline veins in the adjacent eclogite, along which omphacite and garnet are replaced by dark green hornblende, diopside, and plagioclase. These later veins or joints occur even in the freshest eclogites and represent an initial stage of post-eclogite facies overprinting controlled by the access of external fluids (cf. Heinrich, 1982, p. 33).

From a total of about 200 samples studied in thin section, 2 to 6 omphacite + quartz-bearing rocks from 4 areas of less than 1 km^2 each (Gagnone, Trescolmen, Confin and Vals; Fig. 1), plus a few additional samples from other localities in the Adula Nappe, were chosen for electron microprobe investigation. They were selected on the basis of their showing relatively simple textures among 'primary' hydrous and anhydrous silicates, with no or

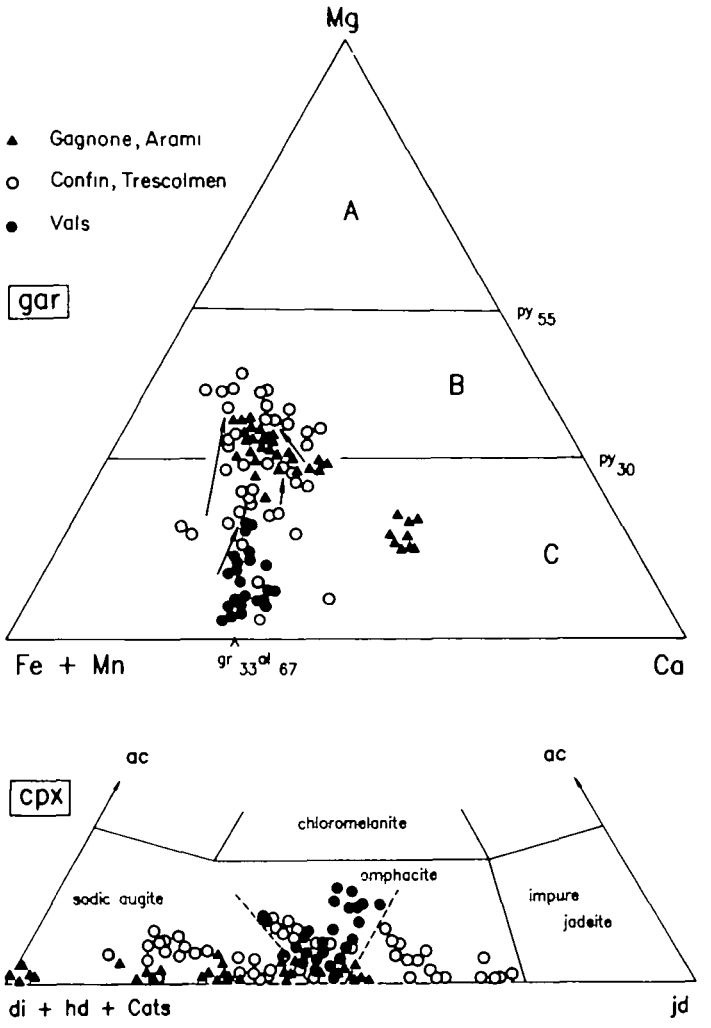

FIG. 3. (*a*, above) Composition of eclogitic garnets, with arrows indicating trends from core to rim of zoned porphyroblasts. Empirical boundaries for mole per cent pyrope (py_{30} and py_{55}) separating type-A, -B, and -C eclogites are from Coleman *et al.* (1965). (*b*, below) Composition of Adula clinopyroxenes in the triangle $di + hd + CaAl_2SiO_6$ (Cats) = Ca, jd = $Na\text{-}Fe^{3+}$, and ac = Fe^{3+}, after Essene & Fyfe (1967).

only traces of incipient retrogression to amphibolitic symplectite textures (Table 1). Representative point analyses are given in Tables 2 and 3 together with analytical and recalculation procedures.

P-T ESTIMATES FROM MINERAL CHEMISTRY OF GARNETS AND PYROXENES

The composition of the anhydrous eclogite minerals, garnet and clinopyroxene (Fig. 3), constrains the pressure-temperature conditions of the formation of quartz-bearing eclogites, independent of the presence of additional hydrous phases.

Fe^{2+}/Mg fractionation between garnet and clinopyroxene

The temperature-dependent exchange equilibrium

$$Fe^{2+}Mg_{-1}(cpx) = Fe^{2+}Mg_{-1}(gar) \quad (1)$$

(vector notation after Thompson, 1981; Thompson *et al.*, 1982) is relatively pressure insensitive, and can be used to estimate the formation temperature of eclogitic assemblages. Fig. 4a is a log-log plot showing the Fe^{2+}/Mg distribution data from the Adula Nappe according to equilibrium (1). Contours for constant distribution coefficients $K_D = 6{\cdot}5$ and $K_D = 17$, where

$$K_D = \left(\frac{Fe}{Mg}\right)^{gar} \Big/ \left(\frac{Fe^{2+}}{Mg}\right)^{cpx},$$

separate empirical K_D ranges for garnet-omphacite pairs from different geological settings as suggested by Banno & Matsui (1965) and Lovering & White (1969). Largely because of changing garnet compositions (Fig. 3*a*), K_D values from the northern and southern part of the Adula Nappe plot in clearly different fields, in general agreement with their present metamorphic environment. Ellis & Green (1979) have calibrated equilibrium (1) as a function of temperature, pressure, and the Ca-content of the system, expressed by the grossular content (X_{Ca}^{gar}). Their equation (9) can be rearranged to

$$\log\left(\frac{Fe}{Mg}\right)^{gar} - \frac{1348}{T}X_{Ca}^{gar} = \log\left(\frac{Fe}{Mg}\right)^{cpx} + \left(\frac{1316}{T} - 0{\cdot}826 + \frac{4{\cdot}72\,P}{T}\right). \quad (2)$$

The left hand term of equation (2) may formally be considered as a garnet composition term, empirically corrected for the non-ideality in garnet. A first approximation for T of 773, 873, 973 and 1073 K for Vals, Confin, Trescolmen and Gagnone/Duria/Arami was used for the correction, which is only weakly dependent on the T values. The garnet composition data thus corrected are shown as a function of $\log(Fe^{2+}/Mg)^{cpx}$ in Fig. 4*b*. The 'Ca-corrected distribution coefficient', K_D^*, is plotted in Figs. 4*b*, 5 and as a function of temperature and pressure in Fig. 6, where:

$$\log K_D^* = \log K_D - \frac{1348}{T}X_{Ca}^{gar}. \quad (3)$$

Fig. 4*b* shows that Ellis & Green's calibration corrects for all compositional effects among the samples from the northern and southern Adula localities, indicating a trend in K_D^* such that:

$$\underset{\text{South}}{K_D^*(\text{Arami, Duria})} < K_D^*(\text{Gagnone}) < \underset{\text{North}}{K_D^*(\text{Vals})}.$$

The distribution coefficients for the intermediate Confin and Trescolmen localities vary considerably even after correction for X_{Ca}^{gar}. K_D^* tends to decrease with increasing jadeite content of the particularly sodic omphacites from each of these two localities (Fig. 5). A similar effect has been found for jadeitic pyroxenes of the Western Alps, where Koons (1984) proposed preferential ordering of Fe relative to Mg into the M2-site of clinopyroxene (solid solution towards clinoferrosilite) as a likely cause for this effect. Koons (1984) suggested that, as the total Fe + Mg in M1 is high (as in the jadeite-poor pyroxenes used in Ellis & Green's experiments), ordering of relatively minor Fe in M2 has no strong effect on the bulk Fe/Mg ratio of the pyroxene. However, the preference of Fe^{2+} for the slightly larger M2 site becomes relatively more important with increasing jadeite content (and hence decreasing total Fe + Mg content) of very sodic omphacites. The shape of the dashed curves in Fig. 5 is calculated to represent the maximum estimated effect of M1, M2 ordering on K_D^*. They were

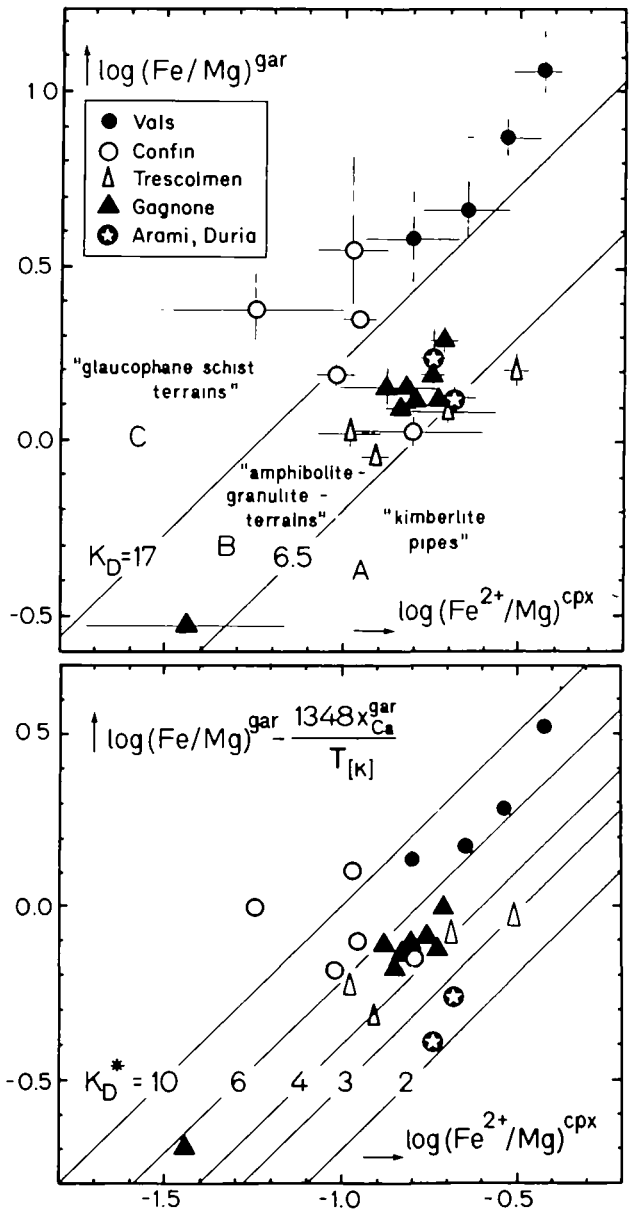

FIG 4. (*a*, above) Logarithmic distribution diagram of Fe^{2+}/Mg between garnets and clinopyroxenes from the Adula Nappe. Fe^{2+}(cpx) is estimated from cation normalized stoichiometry (see Table 2), while for garnet Fe(gar) = Fe^{tot} was plotted neglecting minor ferric iron. Empirical boundaries of $K_D = 6{\cdot}5$ and 17 separating type-A, -B and -C eclogites are from Lovering & White (1969). (*b*, below) The same data as in (*a*), except that the garnet composition term (vertical axis) is corrected for X_{Ca}^{gar} after Ellis & Green (1979) (eqn. (2), text). The Ca-corrected distribution coefficient K_D^*, indicated by the 45° contours, is constant for the mineral pairs from each of the localities Vals, Gagnone and Arami/Duria, but widely variable for pairs from Trescolmen and Confin (see text and Fig. 5).

TABLE 2

Electron microprobe analyses of clinopyroxenes and garnets

Clinopyroxene	*Ad42-9-14*	*Ad65-0-8*	*Ad48-9-5*	*Ad25-9-3*	*Ad61-9-1*	*CH271*	*Mg9-5-12c*
SiO_2	55·17	55·20	55·80	55·14	57·93	56·10	55·33
TiO_2	0·22	0·12	0·00	0·07	0·06	0·06	0·12
Al_2O_3	11·13	11·61	11·12	10·08	17 85	12 62	11·36
Cr_2O_3	0·00	0·00	0·05	0·07	0·03	0·00	0·00
FeO(tot)	4·99	8·01	2·81	2·41	2 62	2 59	3·07
MnO	0·08	0·05	0·00	0·00	0·00	0·00	0·04
MgO	8·00	5·43	8·91	10·43	4 79	8 38	9·27
CaO	13·24	10·15	13·55	15·60	6 84	13·07	14·44
Na_2O	6·81	8·53	6·86	5·47	10·72	7 23	6·33
Total	99·65	99·09	99·10	99·27	100·84	100·04	99·97
Cations normalized to Σ(cations) = 6							
Si	1·97	1·99	1·99	1·97	1 99	1·97	1·96
Ti	0·01	0·00	0·00	0·00	0·00	0·00	0·00
Al(tet)	0·03	0·01	0·01	0·03	0·01	0·03	0·04
Al(oct)	0·44	0·48	0·45	0·39	0·71	0·50	0·43
Cr	0·00	0·00	0·00	0·00	0·00	0·00	0·00
Fe^{3+}	0·05	0·13	0·03	0·01	0·01	0·02	0·04
Fe^{2+}	0·10	0·12	0·05	0·06	0·07	0·06	0·05
Mn	0·00	0·00	0·00	0·00	0·00	0·00	0·00
Mg	0·43	0·29	0·47	0·56	0·25	0·44	0·49
Ca	0·51	0·39	0·52	0·60	0·25	0·49	0·55
Na	0·47	0·60	0·47	0·38	0·71	0·49	0·44

Garnet	*Ad42-9-14 rim*	*Ad65-0-8 rim*	*Ad48-9-5 rim*	*Ad48-9-5 core*	*Ad25-9-3 rim*	*Ad61-9-1 rim*	*CH271 rim*	*CH271 core*	*Mg9-5-12c rim*
SiO_2	38·65	37 55	38 76	38 61	40·05	39 29	39·12	39·51	39·19
TiO_2	0·11	0·12	1 10	0·09	0·04	0·03	0·00	0·15	0·06
Al_2O_3	21·85	20·99	21 81	21 66	22·56	22 82	22 25	22·00	21·89
Cr_2O_3	0·00	0·00	0·06	0·00	0·00	0·00	0·00	0·00	0·00
FeO(tot)	27·35	27·64	21·41	21·04	19·39	22 95	22 87	21·40	18·53
MnO	0·66	0·96	0·26	1 50	0·43	0·00	0·51	0·53	0·47
MgO	3·35	1 54	7·83	5 29	11·17	10·25	9·89	9·01	7·81
CaO	9·81	10·97	8·67	10·70	6·90	5·07	5 88	8·31	11·94
Total	101·79	99 77	99·90	98 87	100·55	100·41	100·52	100·92	99 90
Cations normalized to Σ(cations) = 8									
Si	2·99	3·00	2·96	3 01	2·99	2·97	2 97	2·99	2 99
Ti	0·01	0·01	0·06	0·01	0·00	0·00	0·00	0·01	0·00
Al	1·99	1·97	1·97	1·99	1·99	2·03	1·99	1 96	1·98
Cr	0·00	0·00	0·00	0·00	0·00	0·00	0·00	0·00	0·00
Fe	1·77	1·85	1 37	1·37	1·21	1·45	1 45	1 35	1·18
Mn	0·04	0·07	0·02	0·10	0·03	0·00	0·03	0·03	0·03
Mg	0·39	0·18	0·89	0·62	1 24	1·15	1 12	1·01	0·89
Ca	0·81	0·94	0·71	0·89	0·55	0·41	0·48	0·67	0·98

Single representative point analyses of contacting mineral grains are listed above and in Table 3. Unless indicated otherwise, rim or plateau compositions are given See Table 1 and Appendix 1 for sample description

Analytical conditions: Wave-length dispersive spectrometers on automated ARL-SEMQ microprobe; 15 kV acceleration voltage, 20 nA reference sample current on brass, 20 sec counting time; 10 μm defocussed beam for micas to prevent alkali loss. Simple natural silicate and oxide standards. ZAF-correction, including fixed amounts of H_2O for hydrosilicates (Table 3), using program EMMA (J Sommerauer and R. Gubser, ETH Zürich). Normalization of clinopyroxene analyses to 6 cations (Laird & Albee, 1981, appendix 1) nearly always resulted in fully charge-balanced formulae of ideal site occupancy with slightly less than 2·00 Si per 6 cations, thus allowing unique assignment of Fe^{2+} and Fe^{3+}

calculated for (in atoms per 6 cations): $Fe^{2+}(M2) = 0·04$, $Mg(M2) = 0$, $Fe^{2+}/Mg(M1) = 0·1$. Assuming maximum possible site preference, these values could be representative for the analysed Na-rich omphacites (Ad61-9-1, E5-10; Table 2), indicating that the ordering mechanism proposed by Koons (1984) has the right magnitude to explain the compositional

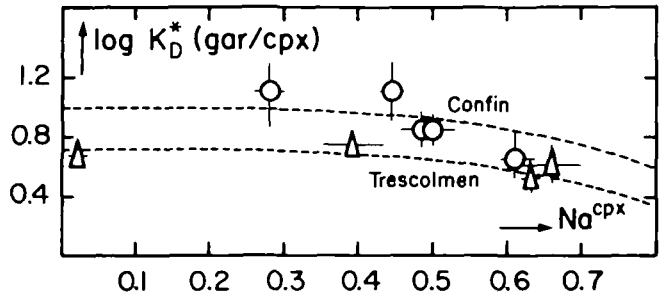

FIG. 5. The compositional dependence of the garnet–clinopyroxene Fe/Mg distribution coefficient remaining after application of the correction for K_D^* by Ellis & Green (1979). Log K_D^* (see eqn. (3), text) tends to decrease with increasing Na-content of the relatively jadeite-rich omphacites from each of the areas Confin (circles) and Trescolmen (triangles). The dashed lines (at arbitrary vertical position) are theoretically calculated to show the maximum effect which preferential Fe^{2+} ordering in the clinopyroxene M2-site is expected to have on log K_D^* (Koons, 1984)

dependence of $\log K_D^*$ observed in the Adula assemblages. Unfortunately the analytical observations scatter too much to place any quantitative limits on this ordering model.

Excluding omphacites with $X_{jd} > 0{\cdot}6$, where cation ordering is more likely to cause systematic errors in temperature estimation, the largest *uncertainty* in applying Ellis & Green's thermometer to Adula eclogites is probably mineral inhomogeneity. Error bars in Figs. 4 and 5 represent the total variation of 5–20 point analyses of several adjacent garnet and pyroxene grains, excluding only the Ca-Fe-rich compositions of inclusion-rich cores of texturally zoned garnet porphyroblasts. The apparent uncertainty could have been reduced by selecting only analyses of rims in immediate contact, a procedure which generally yields the lowest values for K_D^*. However, such a selection could introduce a systematic error, because of the possibility of local post-eclogite Fe/Mg exchange along grain boundaries during amphibolite facies overprinting. With the wider error bars shown in Fig. 4, the total uncertainty due to incomplete chemical equilibrium probably outweighs the errors resulting from stoichiometric estimation of Fe^{2+}/Fe^{3+} in pyroxene, because normalization to 6 cations allowed a unique assignment of cation occupancies to an ideal charge-balanced pyroxene stoichiometry in most cases. Possible exceptions are some clinopyroxenes with very low total Fe/Mg, notably ultramafic garnet peridotites where uncertainties due to stoichiometric Fe^{2+}/Fe^{3+} estimation may be larger than in mafic eclogites (e.g. the point in the lower left corner of Fig. 4 representing the analyses from the Gagnone peridotite given by Evans & Trommsdorff, 1978).

Jadeite content (X_{jd}) of clinopyroxene coexisting with quartz

In combination with Fe–Mg exchange thermometry, the net-transfer equilibrium

$$NaAlSi_2O_6(cpx) = NaAlSi_3O_8(plg) + SiO_2(qtz) \quad (4)$$

places limits on the formation pressure of omphacite + quartz ± albite, but uncertainties due to ordering in omphacite restrict its application to natural assemblages.

Site ordering of Na,Al and Ca,Mg + Fe causes preferential stabilization of clinopyroxenes with compositions close to jadeite : diopside + hedenbergite = 1 : 1, which leads to two miscibility gaps in the system $NaAlSi_2O_6$–$Ca(Mg,Fe)Si_2O_6$ at low temperatures (Clark & Papike, 1968; Carpenter, 1980). Ordering can occur during cooling of originally disordered high-temperature omphacites. Alternatively it may be primary in lower-temperature omphacites from blueschist terrains, in which case it is often reflected by gaps in

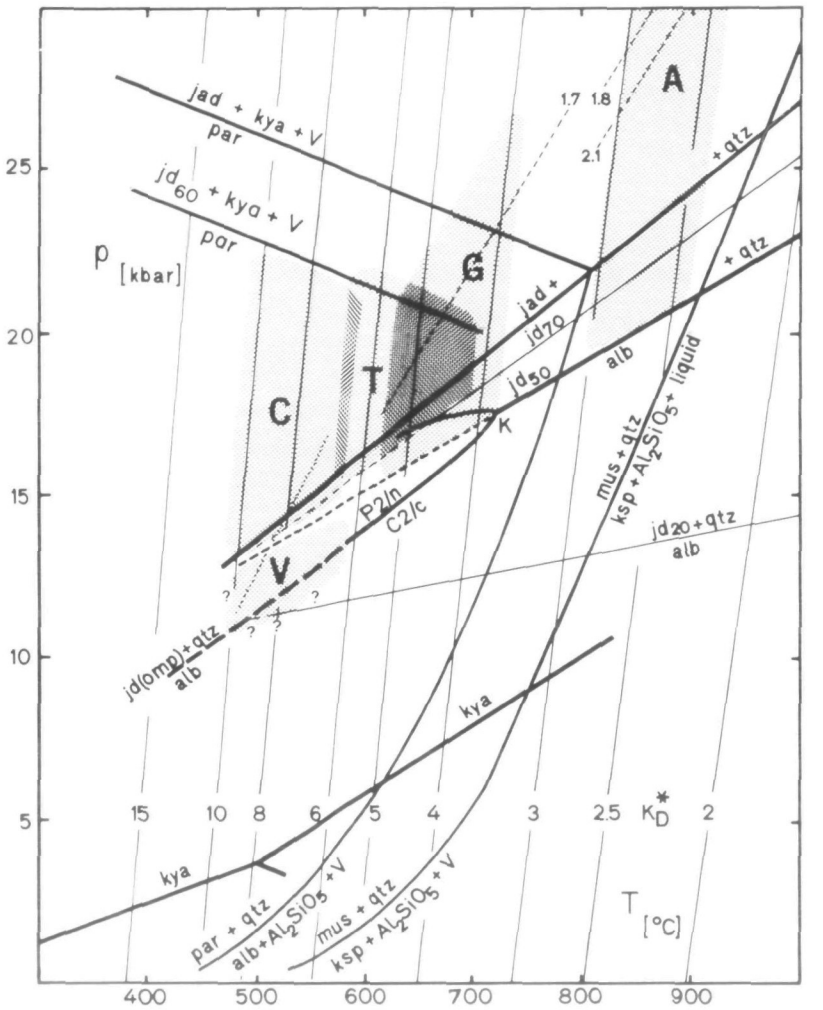

FIG. 6. P-T locations of some experimentally determined equilibria, and likely conditions of crystallization of the quartz + omphacite + garnet assemblages (shaded areas) from Vals (V), Confin (C), Trescolmen (T), Gagnone (G) and Arami/Duria (A). Contours of K_D^* refer to the Ca-corrected distribution coefficient of Fe^{2+}/Mg between garnet and clinopyroxene (eqn. (3), text), after Ellis & Green (1979). Isopleths of jadeite (jd, mole per cent) in omphacite according to equilibrium (4) after Gasparik & Lindsley (1980). The preferred stabilization of ordered P2/n omphacites to pressures below the dashed jd_{50} contour (P2/n–C2/c boundary) is schematic only (cf. Holland, 1983). Dashed contours 1·7, 1·8 and 2·1 are for the Al-contents of orthopyroxenes in garnet lherzolites from Gagnone, Arami and Duria, respectively, from data given by Evans & Trommsdorff (1978), recalculated using the new calibration of Harley & Green (1982). Other curves ($P_{H_2O} = P$) are from Chatterjee & Johannes (1974) for mus + qtz = $Al_2SiO_5 + H_2O$, from Thompson & Tracy (1979) for the minimum melting of muscovite + quartz, from Chatterjee (1972) and Holland (1979*b*) for the reactions involving paragonite, and from Holdaway (1971) for the stability field of kyanite.

compositional plots such as Fig. 3*b* (cf. Carpenter, 1980, fig. 7*b*). Completely ordered omphacites have not been synthesized in laboratory experiments, but Holland (1983) measured at 600 °C the effect of partial ordering on extending the stability field of intermediate omphacite compositions (+quartz) relative to albite. Gasparik & Lindsley (1980) used part of these data to fit the P-T dependence of the mole fraction of $NaAlSi_2O_6$ (X_{jd}) in disordered and partly ordered clinopyroxenes coexisting with albite + quartz. Contours in Fig. 6 are derived from Gasparik & Lindsley (1980, p. 332).

The omphacites from Confin, Trescolmen and Gagnone are acmite-poor and cover the whole compositional range from diopside–hedenbergite to more than 70 mol per cent jadeite (Fig. 3*b*). The absence of any compositional gaps suggests that at least those clinopyroxenes with compositions outside $X_{jd} = 0{\cdot}5 \pm 0{\cdot}1$ have originally crystallized in the disordered C2/c state (cf. Carpenter, 1980, fig. 7*a*). This suggestion is in agreement with the relatively higher equilibration temperatures indicated for the southern parts of the nappe by the Fe/Mg distribution data. The contours for equation (4) according to Gasparik and Lindsley (1980) therefore allow a realistic estimation of the minimum pressures required to stabilize the plagioclase-free eclogites from Confin, Trescolmen and the southern Adula Nappe (Fig. 6).

By contrast, all omphacites from the northern Adula Vals locality plot in a small wedge-shaped field in Fig. 3*b* (dashed lines) with its apex near $X_{jd} = 0{\cdot}5$. Comparison with fig. 7*b* of Carpenter (1980) suggests primary crystallization of the Vals pyroxenes in the ordered P2/n omphacite structure, in agreement with a relatively low crystallization temperature. Because of the unknown effect of complete ordering on stabilizing low-temperature omphacites, the extrapolated jd_{50} isopleth (Fig. 6) after Gasparik & Lindsley probably provides an upper limit for the formation of the omphacite + quartz + albite assemblages from Vals. The true crystallization pressure may be a few kilobars lower, as sketched in Fig. 6 by the qualitative curve jd(omp) + qtz = alb and the shaded area 'V'. Any errors in pressure estimation due to ordering in omphacite would be accentuated if extrapolation of Ellis & Green's Fe/Mg geothermometer caused any over-estimation of crystallization temperatures due to ordering or other non-ideality effects in omphacite and garnet solid solutions. The *P–T* limits for the Vals area are therefore subject to the largest uncertainty.

Al-content of orthopyroxene

Eclogite formation pressures can be further constrained from published Al-contents of orthopyroxenes in garnet lherzolites from Gagnone, Arami and Duria, *if* it is assumed that these rocks formed at the same metamorphic conditions as the associated eclogites. This assumption is debated (Ernst, 1978; Evans & Trommsdorff, 1978) but compatible with the data of Evans *et al.* (1979) and the present eclogite data (Fig. 6). Orthopyroxene from a single occurrence of 2-pyroxene eclogite at Trescolmen has an Al-content below 0·01 atoms per 4 cations, which indicates a lower temperature than for the crystallization of the southern Adula peridotites, but which is too low to sensitively constrain equilibration pressure (Harley & Green, 1982).

Conclusions from thermobarometry

The estimation of absolute values delimiting crystallization conditions of the Adula eclogites involves errors which may be systematic and which are probably larger than commonly assumed. Despite this, the mineral compositions of anhydrous eclogite matrix minerals show a systematic trend of *regional* increase in recorded temperatures and pressures from north to south through the present Adula Nappe. Combining all available data, the following values are considered to be the most likely *P–T* brackets for the matrix recrystallization of eclogitic rocks from different areas of the Adula Nappe:

Vals	450–550 °C	10–13 kb	North
Confin	450–550 °C	12–22 kb	
Trescolmen	550–650 °C	15–22 kb	
Gagnone	600–700 °C	15–25 kb	
Arami, Duria	750–900 °C	18–35 kb	South

TABLE 3

Electron microprobe analyses of primary hydrous silicates and albite

Amphibole	*Ad42-9-14*	*Ad65-0-8*	*Ad48-9-5*	*Ad25-9-3*	*Ad61-9-1*	*CH271*	*Mg9-5-12c*
SiO_2	45·04	54·67	47·70	49·42	58·21	46·29	43·08
TiO_2	0·61	0·08	0·27	0·23	0·10	0·56	0·89
Al_2O_3	14·12	11·18	12·75	12·43	13·82	16·35	15·64
Cr_2O_3	0·00	0·00	0·05	0·05	0·00	0·00	0·07
FeO(tot)	12·26	13·69	8·26	5·68	3·65	6·50	8·04
MnO	0·09	0·08	0·00	0·00	0·00	0·04	0·06
MgO	11·32	8·91	14·70	16·26	13·59	14·30	14·67
CaO	8·76	2·15	9·01	8·90	1·36	7·20	10·73
Na_2O	4·02	6·20	3·41	3·34	7·06	5·20	3·74
K_2O	0·49	0·05	0·32	0·32	0·15	0·75	0·06
H_2O^*	2·50	2·50	2 50	2·50	2·50	2·50	2·50
Total	99·21	99·52	98·97	99·13	100 44	99·67	99·46
Cations normalized to Σ(cations) − Ca − Na − K = 13							
Si	6·55	7·67	6·76	6·89	7·73	6·49	6·16
Ti	0·07	0·01	0·03	0·02	0·01	0·06	0·09
Al(tet)	1·45	0·33	1·24	1·11	0·27	1 51	1·84
Al(oct)	0·97	1·51	0·88	0·93	1·89	1·19	0·80
Cr	0·00	0·00	0·01	0·01	0·00	0·00	0·01
Fe^{3+}	0·39	0·46	0·57	0·51	0·12	0·50	0·50
Fe^{2+}	1·11	1·15	0·41	0·15	0·28	0·26	0·46
Mn	0·01	0·01	0·00	0·00	0·00	0·00	0·00
Mg	2·46	1·86	3·10	3·38	2·69	2·99	3·13
Ca	1·36	0·32	1·37	1·33	0·19	1·08	1·65
Na(M4)	0·64	1·68	0·63	0·67	1·81	0·92	0·36
Na(A)	0·50	0·01	0·30	0·23	0·01	0·49	0·68
K	0·09	0·01	0·06	0·06	0·03	0·13	0·01

Albite, epidote-group minerals and sheet silicates

	alb Ad42-9-14	*clz* Ad42-9-14	*epi* Ad65-0-8	*clz* Ad48-9-5	*zoi* Ad25-9-3	*zoi* Mg9-5-12c	*phe* Ad42-9-14	*phe* Ad25-9-3	*phe* Ad48-9-5	*par* Ad48-9-5	*par* Ad61-9-1	*talc* Ad61-9-1
SiO_2	68·21	38 79	37·68	39·18	39·84	39·24	49·17	51·83	49·17	45·45	46·61	61·14
TiO_2	0·00	0·14	0·11	0·25	0·05	0·06	0·52	0·33	0·41	0·13	0·11	0·00
Al_2O_3	20·01	28·21	26·16	29·61	32·35	32·71	29·52	26·21	28·88	38·82	39·81	0·55
Cr_2O_3	0·00	0·00	0·00	0·03	0·00	0·04	0·00	0·00	0·05	0·03	0·00	0·00
FeO(tot)†	0·15	7·35	9·65	4·59	1·09	1·27	2·39	0·98	1·32	0·46	0·00	6·95
MnO	0·00	0·00	0·11	0·00	0·05	0·00	0·00	0·00	0·00	0·00	0·00	0·00
MgO	0·00	0·14	0·00	0·12	0·09	0·09	2·91	4·63	3·18	0·24	0·17	26·95
CaO	0·78	23·46	23·61	24·62	23·87	23·84	0·01	0·02	0·05	0 53	0·00	0·00
Na_2O	11·35	0·00	0·00	0·00	0·04	0·03	1·31	0·45	1·02	6·97	7·73	0·09
K_2O	0·04	0·00	0·00	0·02	0·00	0·00	9·44	10·21	9·65	0·98	0·18	0·02
H_2O*	0·00	1·80	1 80	1·80	1·80	1·80	4·50	4·50	4·50	4·50	4·50	4·50
Total	100·54	99·89	99·13	100·21	99·18	99 07	99·76	99·16	98·22	98·09	99·10	100·20
Cations												
Si	2·97	2·99	2·95	2·99	3·04	3·00	3·25	3·43	3·30	2·96	2·98	3·96
Ti	0·00	0·01	0·01	0·00	0·00	0·00	0·03	0·02	0·02	0·01	0·01	0·00
Al	1 03	2·57	2·42	2·67	2·91	2 95	2·30	2·04	2·29	2·98	3·00	0·04
Cr	0·00	0·00	0·00	0·00	0·00	0·00	0·00	0·00	0·00	0·00	0·00	0·00
Fe	0·01	0·47	0·63	0·29	0·07	0·08	0·13	0·05	0·07	0·03	0·00	0·38
Mn	0·00	0·00	0·01	0·00	0·00	0·00	0·00	0·00	0·00	0·00	0·00	0·00
Mg	0·00	0·02	0·00	0·01	0·01	0·01	0·29	0·46	0·32	0·02	0·02	2·61
Ca	0·04	1·94	1·98	2·02	1·95	1·95	0·00	0·00	0·00	0·04	0·00	0·00
Na	0·96	0·00	0·00	0·00	0·01	0 00	0·17	0·06	0·13	0·88	0·96	0·01
K	0·00	0·00	0·00	0·00	0·00	0·00	0·80	0·86	0·83	0·08	0·02	0·00

Representative analyses of grains in immediate contact with garnet + omphacite (for analyses see Table 2) + quartz ± kyanite (Table 1; Appendix 1) are given. Amphibole analyses were normalized to a cation sum $\Sigma(\text{cations}) - Ca - Na - K = 13$. Site allotment and estimation of Fe^{2+}/Fe^{3+} using the assumption $(Mg, Fe)^{M4} = 0$ (no anthophyllite-type exchange) mostly resulted in charge-balanced amphibole formulae, in contrast to other possible assumptions (normalization 3 of Laird & Albee, 1981, Appendix 1). The other analyses were normalized to $\Sigma(\text{cations}) = 5$ for albite; $\Sigma(\text{cations}) = 8$ for epidote-group minerals, epidote, clinozoisite, and zoisite; $\Sigma(\text{cations}) - Ca - Na - K = 6$ for the sheet silicates, phengite, paragonite, and talc.

* Assumed for ZAF correction. † As Fe_2O_3(tot) in epidote-group mineral analyses.

In addition to this regional trend, incomplete equilibration as recorded by garnet zoning from Fe-rich cores to Mg-rich rims (Fig. 3*a*) indicates a segment of increasing temperature along the *P-T* path towards crystallization of the matrix assemblage of *individual* eclogites.

MINERAL CHEMISTRY OF PRIMARY ECLOGITIC HYDROSILICATES

Paragonite has been identified by microprobe in eclogites of the northern and central Adula Nappe, usually occurring together with phengite. Its composition is displaced only slightly from the end-member $NaAl_3Si_3O_{10}(OH)_2$ by about 0·1 atom units of KNa_{-1} towards muscovite and an equal displacement along the (negative) Tschermak's vector $-Al_2(Mg,Fe)_{-1}Si_{-1}$. It is often associated with relatively jadeitic omphacites, and its even-grained textural alignment with omphacite clearly shows it to be a primary eclogitic hydrosilicate. The occurrence of coexisting paragonite + omphacite($X_{jd} = 0{\cdot}6$–$0{\cdot}7$) + kyanite according to the equilibrium

$$NaAl_3Si_3O_{10}(OH)_2 = NaAlSi_2O_6(cpx) + Al_2SiO_5 + H_2O \qquad (5)$$

provides an upper limit for the load pressure of eclogite formation in the Confin and Trescolmen areas (Fig. 6; Holland, 1979*b*), irrespective of the presence of any fluid phase.

Phengite, the only potassic mica found as primary constituent in Adula eclogites, is displaced from muscovite towards celadonite by 0·35–0·55 units of $-Al_2(Mg,Fe)_{-1}Si_{-1}$. This exchange is inversely correlated with a 0·2 to 0·1 unit exchange of KNa_{-1} towards paragonite. The $Fe^{2+}Mg_{-1}$ exchange equilibrium between phengite and garnet has been studied experimentally by Krogh & Raheim (1978) and by Green & Hellman (1982) under reducing conditions where $Fe^{2+} = Fe^{tot}$ could be assumed. Natural phengites allow considerable exchange along $Fe^{3+}Al_{-1}$, but since some displacement towards tri-octahedral micas is possible as well, no unambiguous estimation of Fe^{2+}/Fe^{3+} from microprobe analysis is possible. Fe^{tot}/Mg is plotted in Fig. 7, which shows the tendency of

$$K_D^{gar/phe} = \frac{(Fe/Mg)^{gar}}{(Fe/Mg)^{phe}} \qquad (6)$$

to be lower for Trescolmen and Confin than for the Vals samples. This qualitatively indicates a lower equilibration temperature for the latter locality, in general agreement with the regional trend of increasing temperature recorded by garnet–clinopyroxene geothermometry. Absolute temperatures derived from Green & Hellman's calibration of $K_D^{gar/phe}(P,T)$, however, are about 100 °C higher than those estimated with the garnet–pyroxene equilibrium (1). This probably indicates that a considerable part of the iron in the Adula phengites is ferric.

Epidote group minerals (zoisite, clinozoisite, epidote) are widespread as a primary phase in eclogite assemblages throughout the Adula Nappe. Their compositions do not show any simple regional distribution pattern. Garnet amphibolites in the North usually contain Fe-rich clinozoisite, whereas kyanite eclogites at Trescolmen and further south more often contain Fe-poor zoisite. However, more Fe-rich clinozoisite occurs in Ca-enriched metarodingitic eclogites at Gagnone (Evans *et al.*, 1979) and Duria (Heinrich, 1983), indicating that the type of epidote group phase is mainly determined by bulk rock composition. In all areas except Arami and Duria, apparently coexisting pairs of zoisite and more Fe-rich clinozoisite have been observed. Eclogites at Arami contain zoisite as the only primary epidote group mineral.

$Fe^{3+}Al_{-1}$ exchange in epidote group minerals is roughly correlated with that in associated omphacites, as calculated from stoichiometric constraints, giving some credence

to the Fe^{2+}/Fe^{3+} estimation procedure used for omphacite. No such correlation has been found for stoichiometrically estimated Fe^{2+} and Fe^{3+} contents of the eclogitic amphiboles which are therefore considered to be very uncertain.

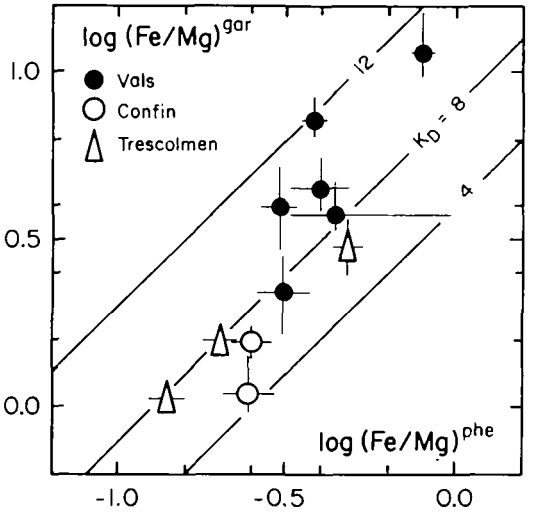

FIG. 7. Logarithmic distribution plot of Fe^{tot}/Mg between garnet and primary phengitic white micas from Vals, Confin and Trescolmen. The open triangle with the highest Fe/Mg value represents the garnet and phengite core of the eclogite facies metapelite from Trescolmen discussed by Heinrich (1982, table 2, sample Ad85).

Amphibole, as a primary eclogitic phase, shows a wide compositional variation, ranging (after Leake, 1978) from impure actinolite in a metadolomite through hornblende, tschermakitic hornblende and barroisite nearly to end-member Mg-glaucophane. The amphibole in most of the mafic quartz eclogites is common hornblende with a ratio of tetrahedral Al to the total octahedral occupancy of $Al + Fe^{3+} + Cr^{3+} + Ti^{4+}$ close to one (Fig. 8*a*). Taken alone, the compositions of the texturally primary eclogitic amphiboles from the Adula Nappe are thus not very different from those of high to intermediate pressure facies series amphibolites (e.g. Laird & Albee, 1981). This observation is in contrast to omphacite assemblages from the Western Alpine Sesia Zone, where amphiboles strongly displaced from glaucophane are restricted to quartz-undersaturated assemblages (Koons, 1982*b*).

Amphibole composition in the Adula eclogites is clearly correlated with the jadeite content of the associated omphacite by the coupled exchange $Na(Al,Fe^{3+})Ca_{-1}(Mg,Fe^{2+})_{-1}$, the jadeite or glaucophane exchange vector (Fig. 8*b*; Heinrich, 1983, figs. 7.3, 7.4). Bulk rock composition is certainly one major control on amphibole and pyroxene composition, but in addition systematic regional differences in mineral compositions are apparent from tie-line rotations such as those shown in Fig. 9. At a given jadeite content of clinopyroxene, the total NaAl-content of the coexisting primary amphibole tends to increase going from the northern to the southern Adula Nappe.

This can be explained by a regional shift in the continuous net-transfer reaction

$$\underset{\substack{\text{jadeite component}\\ \text{in clinopyroxene}}}{NaAlSi_2O_6(cpx)} = \underset{\substack{\text{edenite exchange}\\ \text{in amphibole}}}{NaAl\square_{-1}Si_{-1}(amp)} + 3\ \underset{\text{quartz}}{SiO_2} \qquad (7)$$

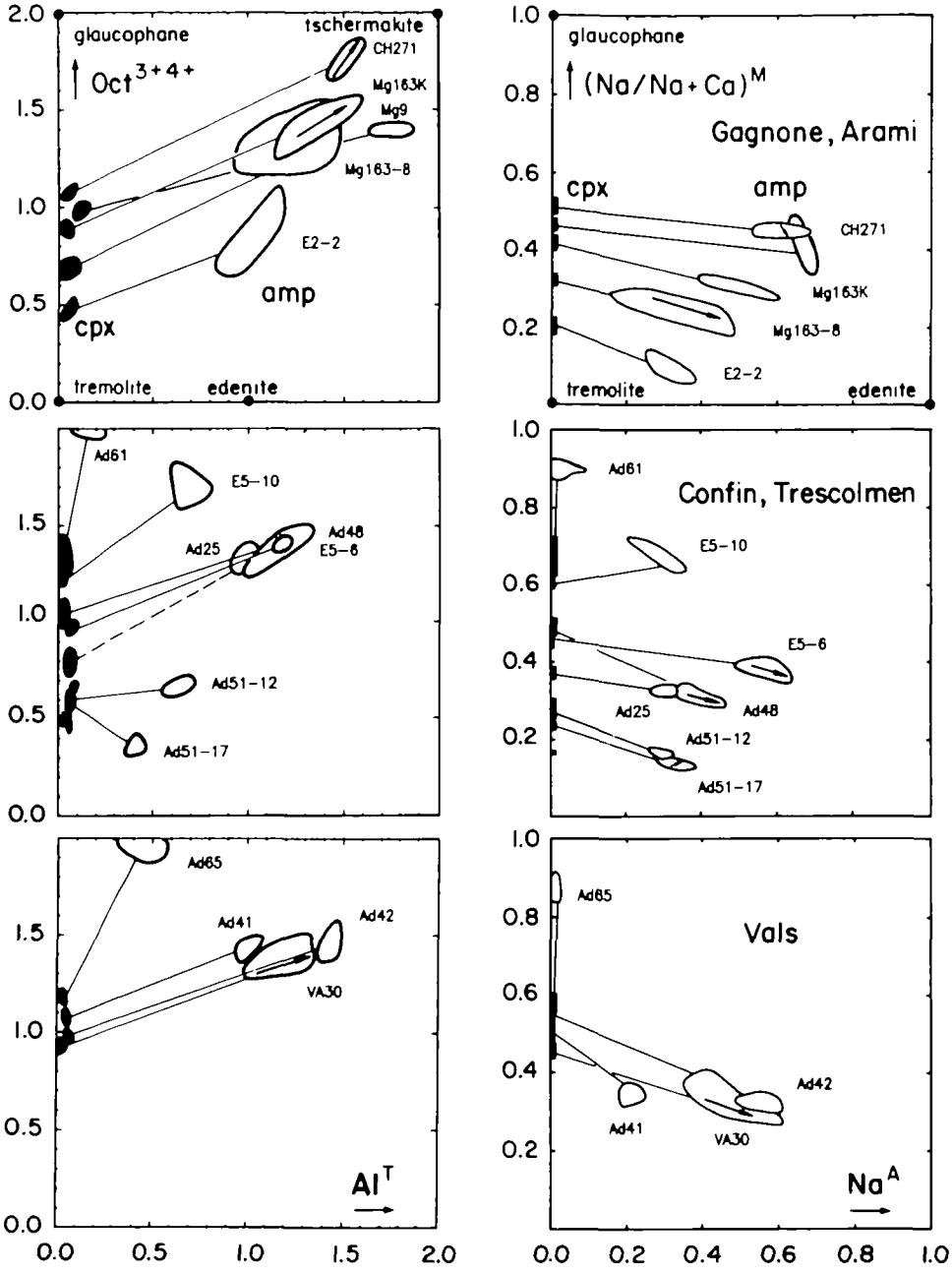

FIG. 8. Mineral composition (in atoms per formula unit, Tables 2 and 3) of primary amphiboles (open symbols) and coexisting clinopyroxenes (full symbols and black bars) in quartz-bearing mafic rocks. Each symbol outlines the full composition range of between 5 and 20 point analyses per mineral and per sample. Arrows indicate zonation trends from grain core to rim. The positions of some important NCMASH end-members of amphibole are indicated for comparison. (*a*, left column) Total octahedral occupancy, $Oct^{3+4+} = Al^{oct} + Fe^{3+} + Cr^{3+} + Ti^{4+}$, versus tetrahedrally coordinated Al. (*b*, right column) Plots of $(Na/Na+Ca)^{M4}$ and $(Na/Na+Ca)^{M2}$ of coexisting amphiboles and clinopyroxenes, respectively, on the vertical axis (measuring the jadeite or glaucophane exchange vector, $Na(Al,Fe^{3+})Ca_{-1}(Mg,Fe^{2+}_{-1})$, versus Na^{A} in amphibole on the horizontal axis (edenite exchange, $NaAl\square_{-1}Si_{-1}$).

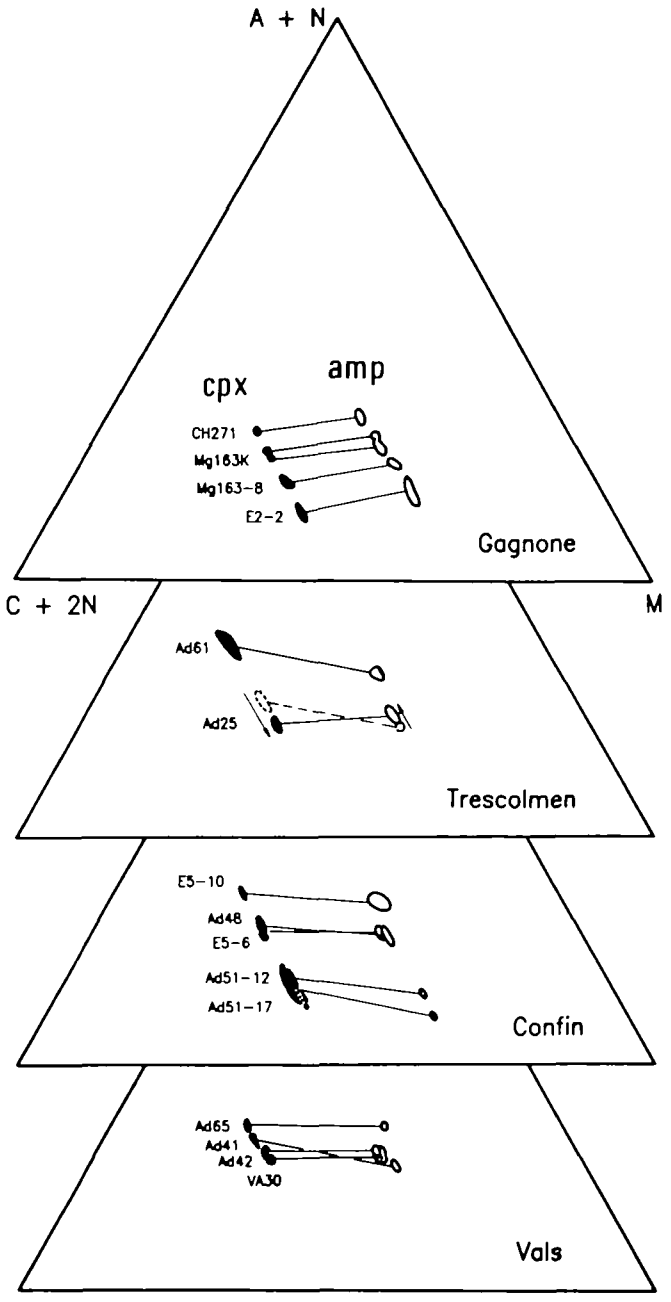

FIG. 9 Coexisting amphiboles (open symbols) and clinopyroxenes (full symbols) in the '*ACF-deluxe*' diagram of Thompson (1981, fig. 28). The coordinates

$$A+N = Al_2O_3+Fe_2O_3+Cr_2O_3+TiO_2+(Na_2O+K_2O)$$
$$C+2N = CaO+2(Na_2O+K_2O)$$
$$M = MgO+FeO+MnO$$

correspond to a projection along the exchange vector $NaSiCa_{-1}Al_{-1}$ (plagioclase vector). Amphiboles from the southern Adula Nappe (Gagnone) coexisting with a clinopyroxene of a given jadeite content tend to be more NaAl-rich than those in the central and northern part of the nappe (notably Confin). In addition to this regional trend, a similar tie-line rotation is also recorded by grain zonations in individual eclogite samples (e.g. Ad25-9-3 from Trescolmen, indicated by arrows).

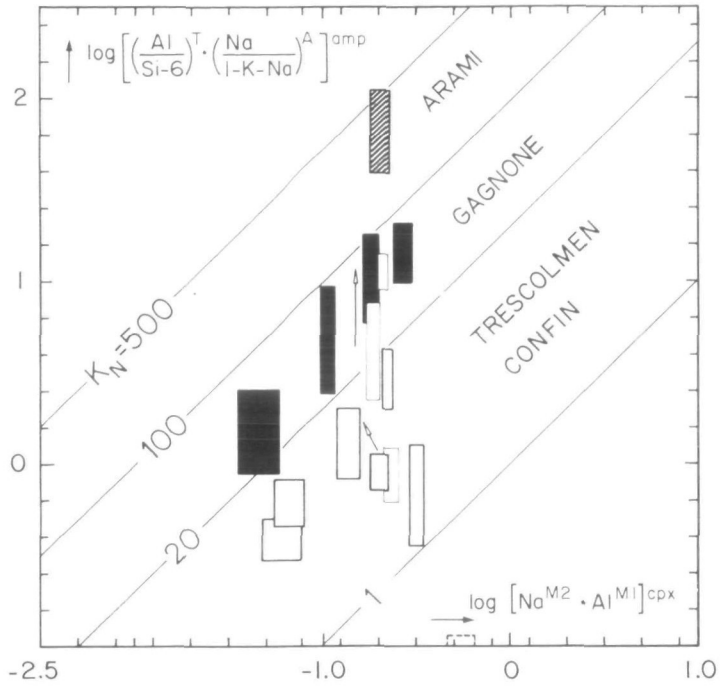

FIG. 10. Log–log diagram for the net-transfer equilibrium (7) showing analytical data of coexisting clinopyroxenes and amphiboles from quartz-saturated assemblages. Equilibrium (7) controls the edenite exchange in amphiboles ($NaAl\square_{-1}Si_{-1}$, vertical axis) as a function of the jadeite content of the coexisting clinopyroxene (horizontal). Glaucophane Ad61-9-1 plots below the diagram because its very low Al^{tet} and Na^{A} is not well constrained by the analysis. The systematic regional differences in K_N probably reflect a regional increase in temperature from north to south recorded by the hydrous eclogite assemblages (see text).

(where □ denotes a vacancy in the A-site of the amphibole). The logarithmic mass-action constant

$$\log K_N = \log \frac{a^{amp}_{NaAl\square_{-1}Si_{-1}} \cdot (a^{qtz}_{SiO_2})^3}{a^{cpx}_{NaAlSi_2O_6}} \tag{8}$$

can be approximated for analysed pairs of amphiboles and clinopyroxenes (coexisting with excess quartz) by

$$\log K_N \simeq \log \frac{\left[\left(\frac{Al}{Si-6}\right)^{tet} \cdot \left(\frac{Na}{1-K-Na}\right)^{A}\right]^{amp}}{[(Na^{M2} \cdot Al^{M1})]^{cpx}} \tag{9}$$

where the element symbols refer to atoms per formula unit in the crystallographic site indicated by the superscript (cf. Tables 2, 3). In Fig. 10, numerator *vs.* denominator of this expression are plotted logarithmically, with contours of constant K_N indicated by the diagonal lines. Alternative ways could be used to express K_N for a given pair of analyses, but the diagram shows qualitatively the regional shift of equilibrium (7) from more jadeitic clinopyroxenes in the northern and central parts of the Adula Nappe (Confin, Trescolmen) to more edenitic amphiboles in the south (Gagnone and Arami).

The edenite exchange in amphiboles from Vals (boxes outlined with fine lines) does not

seem to be effectively controlled by the composition of the coexisting clinopyroxene, probably because the latter is fixed near jd_{50} by preferential stabilization due to ordering (see Fig. 3*b*).

Equilibrium (7) is the high-pressure equivalent of the equilibrium

$$\underset{\text{albite component in plagioclase}}{NaAlSi_3O_8(plg)} = \underset{\text{edenite exchange in amphibole}}{NaAl\square_{-1}Si_{-1}(amp)} + 4\ \underset{\text{quartz}}{SiO_2} \qquad (10)$$

which controls the edenite exchange in amphiboles of quartz-bearing amphibolites at pressures below the breakdown of plagioclase to pyroxene. Laird (1980) and Spear (1981) observed that $NaAl\square_{-1}Si_{-1}$ increases in plagioclase–quartz–amphibole assemblages with increasing metamorphic temperature. From this and the small volume change associated with reaction (7) ($\Delta v^0(7) = -1{\cdot}08$ J bar^{-1} mole^{-1}; using data from Helgeson *et al.*, 1978) it can be predicted that the high-pressure equilibrium (7) is essentially temperature-sensitive only, shifting to the right with increasing temperature. The systematic regional change in the reaction coefficient K_N of reaction (7) indicated by Fig. 10 is therefore in good agreement with the regional gradient in temperature recorded by Fe/Mg exchange between garnet and clinopyroxene.

Where large hornblende poikiloblasts are compositionally zoned, this always involves an increase in tetrahedrally coordinated Al and the ratio Na^A/Na^{M4} from core to rim (Fig. 8). This indicates a trend of increasing K_N (7) (and therefore probably an increase in temperature) during their growth.

Conclusions from mineral chemistry

Comparison of the compositional variations in texturally 'primary' eclogitic hydrosilicates and associated garnets and clinopyroxenes has shown:

(a) a general *correlation* between the compositions of hydrous and anhydrous minerals in rock suites from small areas of the Adula Nappe, indicating bulk rock compositional control in isofacial, often high-variance assemblages;

(b) *regional* shifts in continuous solid-solid equilibria involving 'primary' hydrosilicates, which qualitatively agree with regional differences in crystallization temperatures and pressures recorded by mineral equilibria among the anhydrous eclogite minerals;

(c) *zoning* patterns in 'primary' amphiboles which are compatible with zoning in garnet, both probably recording a path segment of increasing temperature during recrystallization of individual eclogites.

In support of the textural evidence, the mineral chemistry indicates that the crystallization of the 'primary' hydrosilicates is closely linked, and grossly coeval, with the crystallization of the anhydrous eclogite phases.

PHASE RELATIONS IN HYDROUS QUARTZ ECLOGITES

Analysis of phase relations and accurate deduction of mineral reactions between hydrous eclogitic assemblages requires at least *ten* system components: SiO_2, TiO_2, Al_2O_3, Fe_2O_3, FeO, MgO, CaO, K_2O, Na_2O, and H_2O; neglecting minor MnO, Cr_2O_3 and trace elements. Quartz and rutile are the only two phases which are in excess in all the studied samples, and which therefore allow a thermodynamically valid projection in the sense of Greenwood (1967, 1975). For the Adula eclogites, K_2O can be neglected, because its amount in the rock is reflected by the amount of potassic white mica alone, if the small exchange of KNa_{-1} in

amphibole and paragonite is neglected. Further reduction of components can be achieved by combination of components or *condensation* along exchange vectors (Thompson *et al.*, 1982). Condensation of FeO + MgO corresponds to a projection along the exchange vector $FeMg_{-1}$, but this is a thermodynamically valid projection only if the two components do not preferentially fractionate between the phases under discussion, i.e. if they in fact behave like a single component. Although approximately true in the case of the $FeMg_{-1}$ exchange between clinopyroxene and amphibole, this prerequisite obviously does not hold for garnet which is preferentially enriched in Fe and has therefore been excluded from the analysis. This omission may be the most serious limitation in a more general application of the Schreinemakers analysis developed below, but it will not affect the main conclusions.

For a graphical representation of the phase relations in the condensed NCMASH model system (Thompson *et al.*, 1982), two additional projections are necessary. The approach used here is to project tentatively from H_2O and along the $Fe^{3+}Al_{-1}$ vector into the tetrahedron NCMA, where

$$N = Na_2O + K_2O$$
$$C = CaO$$
$$M = MgO + FeO$$
$$A = Al_2O_3 + Fe_2O_3 \quad \text{(Fig. 11).}$$

As a consequence, any reaction relationships apparent from NCMA chemographies of observed assemblages (Fig. 12) will have to be discussed in terms of differences in temperature and pressure, as well as the level of the activities (a) or chemical potentials (μ) of H_2O and $Fe^{3+}Al_{-1}$.

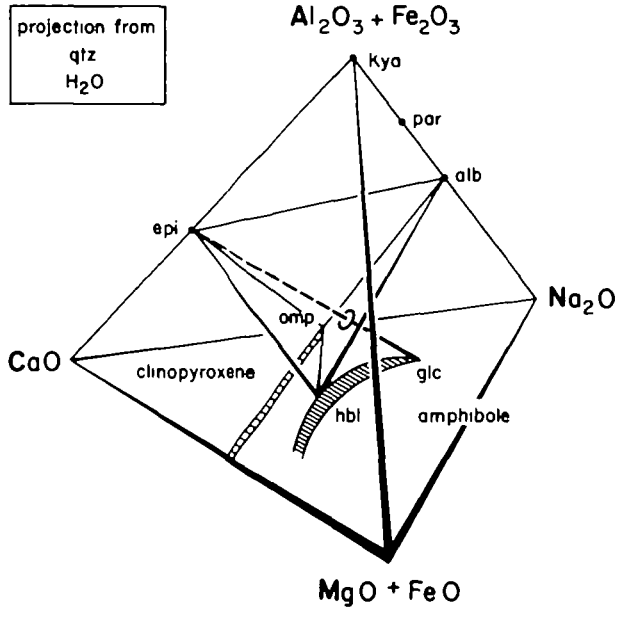

FIG. 11. Perspective representation of primary minerals of Adula quartz eclogites in the NCMA tetrahedron. In addition to projection from quartz and condensation along the exchange vectors $Fe^{2+}Mg_{-1}$ and $Fe^{3+}Al_{-1}$, the tetrahedron involves projection from H_2O, despite the indication from phase relations that the activity of H_2O is not externally controlled in the Adula assemblages, as discussed in the text. The internal tetrahedron hbl-epi-alb-omp represents the common amphibolite assemblage in the Vals area of the northern Adula Nappe. Glc + epi (dashed line intersecting the plane hbl + alb + omp) occurs as an alternative assemblage in the same area, probably due to higher levels of $Fe^{3+}Al_{-1}$ in some rock compositions (see text).

Topological constraints from Schreinemakers analysis

Disregarding initially the compositional variations along $Fe^{3+}Al_{-1}$, and neglecting complications which may arise from miscibility gaps in pyroxenes and possibly other phases at low temperature, the condensed NCMASH-species hornblende, omphacite, epidote (including zoisite/clinozoisite), paragonite, albite, kyanite, quartz and H_2O are related by six reactions. The stoichiometry of these reactions is given in Table 4 for a set of representative condensed phase compositions. Stoichiometric coefficients vary somewhat according to amphibole and omphacite compositions. However, their sign, and hence the topology of the deduced Schreinemakers grid (Fig. 12), does not change within the full range of phase compositions observed in the quartz-bearing assemblages of the Adula Nappe. Among the six reactions only the degenerate reaction

$$\text{par} + \text{qtz} = \text{alb} + \text{kya} + H_2O\ [\text{omp, hbl, epi}] \qquad (11)$$

in the NASH-subsystem has been tested experimentally by Chatterjee (1972) and constrained at higher pressures by the experiments of Holland (1979*b*). Due to a lack of thermodynamic data and the complexity of the amphibole solid solution (Heinrich, 1983, p. 130) the reactions involving hornblende cannot be estimated. Only the sign of their slopes can be realistically inferred by combining the principles of Schreinemakers (e.g. Zen, 1966), approximate calculations of reaction volumes (Table 4), and the assumption that reaction entropies are dominated by H_2O-liberation and (for the H_2O-conserving reaction) by the octahedral to tetrahedral coordination change of Al (cf. Holland & Richardson, 1979). Fig. 12 shows possible relative positions of the six reactions as heavy lines in a P-T diagram.

Unless a_{H_2O} is fixed externally (e.g. by the presence of a hydrous fluid), only the reaction $[H_2O]$ is univariant (and hence truly discontinuous in the 6-component model system NCMASH), because it involves 7 solid phases. These minerals uniquely fix $\mu^*_{H_2O}$ and all mineral compositions at any given point along the line $[H_2O]$. The variation of these parameters along the line $[H_2O]$ is exemplified by its intersection with contours for constant a_{H_2O} as fixed by the equilibrium $\text{par} + \text{qtz} = \text{alb} + \text{kya} + H_2O$ (fine broken lines), and with contours for constant X_{jd} in omphacite as fixed by the equilibrium $\text{alb} = \text{jad} + \text{qtz}$ (fine full lines). Note that the increase of X_{jd} along $[H_2O]$ with falling temperature suggested by the intersecting contours is arbitrary; $[H_2O]$ could equally well have a steeper slope than the jadeite-contours, in which case the variation would be reversed.

The other five H_2O-involving reactions [alb], [kya], [qtz], [par] and [omp, hbl, epi] are divariant bands even in the NCMASH model system, unless a_{H_2O} is given a specified value. Correspondingly, the point I will shift to lower temperatures along the line $[H_2O]$ as a_{H_2O} is lowered. In Fig. 12 the point I and the H_2O-involving NCMASH-reactions are placed arbitrarily to represent positions which would be compatible with $a_{H_2O} \simeq 0{\cdot}5$.

Comparison with natural assemblages

The derived Schreinemakers topology is in agreement with the phase assemblages observed in the four areas Gagnone, Trescolmen, Confin and Vals (shown as the tetrahedral insets in Fig. 12), as well as with the thermobarometric results (indicated by V, C, T, G; cf. Fig. 6). Except for minor tie-line rotations reflecting regional shifts in continuous reactions, the chemographies for *Gagnone* and *Trescolmen* are similar, with kyanite occurring in sufficiently aluminous rocks. An additional epidote phase (usually zoisite) is common in both areas in relatively calcic, typically mafic rock compositions, coexisting with an aluminous hornblende. In more sodic compositions, kyanite + omphacite + quartz coexist with paragonite and glaucophane in the Trescolmen area. The latter minerals have

TABLE 4

Reactions between hydrous and anhydrous phases of mafic quartz eclogites in the condensed NCMASH system

Phase	NCMASH-condensed composition	v^0 (J bar^{-1})	Reference	Stoichiometric coefficients in reactions (Fig 12) [omp] [hbl] [epi]	[kya]	[H_2O]	[alb]	[par]	[qtz]
qtz	SiO_2	2 27	(R)	−1	−6	+4	−4	+1	
kya	Al_2SiO_2	4 41	(R)	+1		+2	+10	+5	+6
alb	$NaAlSi_3O_8$ (low-alb)	10·01	(R)	+1	+10	−8		−5	−4
omp	$Na_{.5}Ca_{.5}Al_{.5}Mg_{.5}Si_2O_6$	6 32	(R)		−14	+14	+14	+14	+14
epi	$Ca_2Al_3Si_3O_{12}(OH)$ (zoi)	13 59	(He)		+2	−2	−2	−2	−2
par	$NaAl_3Si_3O_{10}(OH)_2$	13 20	(Ho)	−1	−5	+3	−5		−1
hbl	$\square_{.5}NaCa_{1.5}Mg_{3.5}Al_{3}Si_{6.5}O_{22}(OH)_2$	26·91	(He, K)		+2	−2	−2	−2	−2
V	H_2O	1·85	(DH)	+1	+2		+8	+3	+4
	estimated volume change Δv^0 (J bar^{-1})			0·80	+16·7	−15 1	−8 6	−12 7	−11 9

Omphacite composition in all Adula rocks containing a calcic (hornblende, epidote) plus a sodic/aluminous phase (albite, kyanite, paragonite) is close to jadeite$_{50}$diopside$_{50}$. Amphibole has been idealized to a hornblende formula hbl = 0·5 tremolite + 0·5 pargasite + 0·5 $NaAlCa_{-1}Mg_{-1}$ + 0·5 $Al_2Mg_{-1}Si_{-1}$, which closely approaches the condensed composition of hornblendes coexisting with jadeite$_{50}$–omphacites.

Molar volumes have been estimated using data from (He) = Helgeson *et al.* (1978), (R) = Robie *et al* (1979), (Ho) = Holland (1979*b*) and (K) = Koons (1982*a*), neglecting non-ideal mixing in omphacite and amphibole. The volume for H_2O is taken from DH = Delany & Helgeson (1978) at the somewhat arbitrary conditions of 12 kb/700 °C, but variation of $v^0(H_2O)$ within the range of equilibration conditions of the Adula Nappe has only a small influence on Δv^0 of the reactions

not been found in Gagnone, although they would be compatible with the observed topology, and also with the estimated P–T conditions and the experimental stability of glaucophane + paragonite (Koons, 1982*a*). Their absence is more likely a consequence of selective overprinting of these assemblages during subsequent amphibolite facies metamorphism (Heinrich, 1982), rather than a reflection of the differences in original eclogite facies P–T conditions between the two areas.

Among the assemblages from *Confin*, a reaction relationship

$$\underset{\text{(Ad48-9-5)}}{\text{par} + \text{epi} + \text{hbl} + \text{qtz}} = \underset{\text{(E5-10)}}{\text{omp} + \text{kya} + H_2O\ [\text{alb}]} \qquad (12)$$

is evident from tetrahedron 'C' (Fig. 12), which must involve H_2O to be balanced. Since the two incompatible assemblages occur in the same eclogite lens, sharing a pronounced mineral lineation, crystallization under different conditions of P and T is unlikely. Amphibole and omphacite in the two samples have similar and low total Fe-contents, and therefore bulk compositional differences with regard to $Fe^{2+}Mg_{-1}$ and $Fe^{3+}Al_{-1}$ are an equally unlikely explanation for the different assemblages. Most probably the two assemblages indicate local differences in the activity of H_2O. The assemblages from Confin are represented in Fig. 12 by the Schreinemakers sector [alb, H_2O], whereby the assemblage omp + kya is stabilized relative to par + epi + hbl + qtz by a shift of reaction [alb] due to a lower level of a_{H_2O}.

The northern Adula Nappe, including *Vals*, is known for its occurrences of mafic rocks with glaucophane. Throughout this area, glaucophane is invariably associated with Fe-rich, true epidote (e.g. Ad65-0-8, Table 3; Gansser, 1937; Plas, 1959; Oberhänsli, 1978). Wherever present, coexisting omphacite is distinctly apple green in thin section indicating a high acmite content (Table 2). The coexistence of glaucophane and a pure CaAl-phase like zoisite or lawsonite, considered diagnostic of the blueschist facies and common in mafics from the

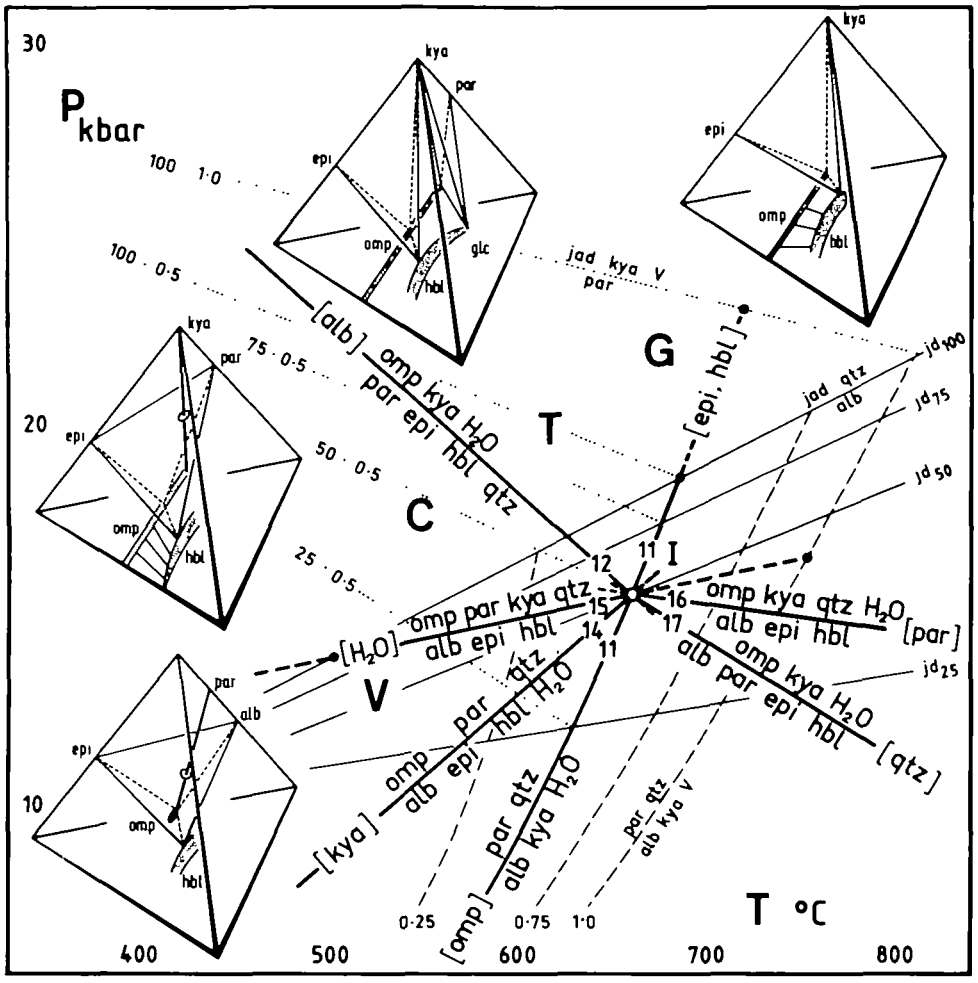

FIG. 12. Partly schematic P-T diagram showing the relative position of some equilibria among NCMASH-condensed minerals of quartz-bearing hydrous mafic rocks (heavy lines; see Table 4 for stoichiometry), in comparison with observed mineral assemblages (tetrahedral chemographies in the projection of Fig. 11) and their approximate crystallization conditions derived from mineral compositions for the localities Vals (V), Confin (C), Trescolmen (T) and Gagnone (G) (Fig. 6). Full fine lines = contours of constant jadeite content (100 X_{jd}) for all assemblages containing albite + omphacite; equilibrium (4). Broken lines = constant a_{H_2O} in assemblages containing paragonite + albite + kyanite + quartz; equilibrium (11) Stippled lines = contours for constant product (100 $X_{jd} \cdot a_{H_2O}$) for assemblages containing par + omp + kya; equilibrium (5). H_2O activites refer to a standard state with $a_{H_2O} = 1$ for the pure aqueous fluid, irrespective of the physical state of the component H_2O.

Sesia zone (Western Alps; Koons, 1982*b*) or in the Franciscan terrain (California; Brown & Bradshaw, 1979), has never been observed in the Adula Nappe.

Glaucophane-epidote rocks in Vals are relatively subordinate to the more common (±omphacite-bearing) garnet-epidote-albite amphibolites in this area. In condensed NCMASH space, the glaucophane and amphibolite assemblages appear to overlap (Fig. 11), linked by the reaction

$$\text{glc} + \text{epi} = \text{alb} + \text{omp} + \text{hbl} + \text{qtz} + \text{H}_2\text{O}. \qquad (13)$$

It is possible that this equation again reflects different values of H_2O activity between

cofacial rocks. However, $Fe^{3+}Al_{-1}$ strongly fractionates between these minerals, with the sequence

$$FeAl_{-1}(epi) \gg FeAl_{-1}(hbl) \simeq FeAl_{-1}(omp) \simeq FeAl_{-1}(glc) \gg FeAl_{-1}(alb)$$

estimated from microprobe analyses. Using non-condensed mineral compositions from the representative samples Ad42-9-14 and Ad65-0-8 (Tables 2, 3), a numerical test of reaction (13) using the method of Greenwood (1967, 1975) has shown that the two assemblages do *not* have overlapping phase polyhedra in multicomponent space also including Fe_2O_3. Glaucophane–epidote assemblages in northern Adula Nappe thus reflect relatively Fe^{3+}-rich bulk compositions, and therefore *not necessarily* different P-T-a_{H_2O} conditions, compared to the more common epidote–albite amphibolite assemblages in the same area. Glaucophane (+epidote) assemblages are not considered explicitly in the following discussion, but the inclusion of this amphibole with 'hbl' would not alter the topology of Fig. 12.

In contrast, the association paragonite+omphacite found in the impure dolomite Ad41-9-20 from Vals is related to the more common epidote–amphibolite assemblages in this area by

$$\underset{(Ad41\text{-}9\text{-}20)}{omp + par + qtz} = \underset{(Ad42\text{-}9\text{-}14)}{alb + hbl + epi} + H_2O\ [kya]. \qquad (14)$$

This relation was also tested numerically, including garnet approximating the analysed compositions. The result showed a small amount of garnet to be involved on the left side of the reaction, but the sign of H_2O and the other solid did not change. Since all phases have very similar compositions in the two samples Ad41-9-20 and Ad42-9-14, the relation (14) indicates local differences in a_{H_2O} as the most likely cause for the different mineral assemblages. Note that the typical assemblage of the carbonate-poor or carbonate-free amphibolites from Vals indicates the lower level of H_2O activity, whereas the dolomite- and calcite-rich schist Ad41-9-20 contains the assemblage indicating the higher H_2O activity. This is in agreement with the interpretation discussed below, that a mechanism other than fluid dilution by CO_2 was the main cause for local variations in μ_{H_2O} during high-pressure metamorphism of the northern Adula Nappe.

In the Schreinemakers grid of Fig. 12, the Vals assemblages are compatible with the sector [kya, H_2O], provided that the less hydrous assemblage alb + epi + hbl is stabilized relative to omp + par by a shift of reaction [kya] (14) due to a lower level of H_2O activity.

It is interesting to conclude that among probably isofacial samples from Vals, which have a mineralogical range transitional between epidote amphibolite and eclogite facies, the 'eclogitic' assemblage omphacite + paragonite (+garnet) is stabilized, not destabilized as perhaps expected, by increased H_2O activity relative to the typical amphibolite assemblage alb + hbl + epi. A similar conclusion has been reached by Brown & Bradshaw (1979) for omphacite in hydrous rocks transitional between lawsonite-blueschist and low-temperature eclogite facies in California.

Isograds of high-pressure metamorphism

The general compatibility of the observed phase topologies with the theoretical Schreinemakers analysis and the thermobarometric results shows that the reactions [alb] and [H_2O] have the character of isograds of high-pressure regional metamorphism. The fact that these 'isograds' are not separated by sharply defined geographic boundaries is a direct consequence of the variations in water activity indicated by isofacial assemblages from Vals

and Confin, but it probably also reflects the low sampling density and the complications by post-eclogite facies deformation. The following interpretation of the geological meaning of these 'isograds' and the physical significance of the reduced water activities in Adula high-pressure metamorphism is therefore tentative.

FLUID PRESENCE AND FLUID ABSENCE IN ADULA HIGH-PRESSURE METAMORPHISM

Metamorphism is often assumed to be a process involving the ubiquitous presence of a free phase. In principle, local and large-scale differences in fluid composition could be invoked to explain the local and regional differences in eclogite mineralogy observed in the Adula Nappe. However, the combined geological, textural, and mineralogical information is explained more easily by a process involving a regional change from fluid-absent to fluid-present high-pressure metamorphism, in response to different P–T paths experienced by different parts of the present Adula Nappe.

The majority of the mafic high-pressure assemblages in the *northern* part of the Adula Nappe (Vals to Confin) formed from high-grade amphibolites, i.e. from hydrous protoliths which had already been dehydrated to some extent by Pre-Alpine metamorphism. As a consequence, high-pressure metamorphism was probably dominated by *H_2O-conserving* reactions forming garnet + omphacite-bearing epidote–albite amphibolites and hydrate-rich eclogites. Their high-pressure mineralogy was in part determined by the bulk hydrate content of the original protolith, in the way generally discussed by Thompson (1955, p. 99). Large-scale differences in recorded P–T conditions within this region of H_2O-conserving metamorphism are now reflected by the geographic distribution of mineral assemblages which are regionally separated by a H_2O-conserving 'isograd' reaction:

$$\text{alb} + \text{epi} + \text{hbl} = \text{omp} + \text{kya} + \text{par} + \text{qtz}\ [H_2O]. \qquad (15)$$

As a consequence of largely H_2O-conserving mineral reactions among H_2O-undersaturated assemblages, high-pressure metamorphism for the majority of the mafic rocks in the northern Adula nappe probably occurred without saturation of the grain boundaries with a free fluid phase. The predominance of *fluid-absent* metamorphism (in the sense of Thompson, 1983), inferred for the northern Adula Nappe, not only explains a_{H_2O} gradients over small distances, but is compatible with the often incomplete recrystallization and generally fine grain size of most high-pressure assemblages in this area. Fluid presence during high-pressure metamorphism of the northern Adula Nappe was probably restricted to the subordinate Mesozoic metasediments (such as the paragonite- and omphacite-bearing carbonate schist Ad41-9-20, see above) which had not been metamorphosed previously, and to localized veins crosscutting some of the older rocks.

In contrast to the water-conserving isograd within the northern Adula Nappe, the reaction separating the phase topology of Confin from that of the *southern* Adula Nappe (e.g. Trescolmen, Gagnone) involves major dehydration:

$$\text{par} + \text{epi} + \text{hbl} + \text{qtz} = \text{omp} + \text{kya} + H_2O. \qquad (12)$$

This dehydration 'isograd' is interpreted to mark the transition from an area of dominantly H_2O-conserving metamorphism in the north to an area further south, where a similar suite of hydrous mafic protoliths reacted by *prograde dehydration* metamorphism to kyanite eclogites, which still contain some primary hydrosilicates but in lower modal abundance. The absence of mineralogical indications for local differences in a_{H_2O} between cofacial eclogites in the southern Adula Nappe indicates that reaction (12) also marks the regional transition

from largely water-undersaturated metamorphism to a metamorphic process during which a_{H_2O} was controlled externally by the rate of dissipation of water from the site of its production (Thompson, 1955, p. 96). Eclogite formation in the southern Adula Nappe probably involved the *local* and *temporary* presence of an H_2O-bearing *fluid* phase.

Local coexistence of the product assemblage of reaction (12) with a macroscopic fluid is shown by quartz veins containing omphacite + kyanite. These veins are particularly frequent at Trescolmen, where also the coarsest-grained eclogites in the Adula Nappe are found. The absence of any wall rock alteration adjacent to these veins, and the presence of all matrix minerals of the kyanite eclogites immediately adjacent to the vein walls are compatible with a stage of fluid presence not only in the veins, but probably also in the mafic eclogites themselves. The veins are interpreted as hydraulic fractures representing the collecting channelways of escaping volatiles produced during eclogite formation (cf. Walther & Orville, 1982). From this it would be expected that the fluids forming the veins at Trescolmen were H_2O-rich, but no primary fluid inclusions have been identified which would allow a direct estimation of the composition of the vein-forming fluid.

Outside the mafic eclogite lenses, fluid-present metamorphism was probably not regionally extensive, even during dehydration of the high-grade mafic eclogites. If the genetic interpretation of a Variscan high-grade pre-metamorphosed basement unit being subjected to subduction metamorphism is correct, then any water produced by eclogitization of mafic amphibolite layers was probably consumed by paragonite- and phengite-forming hydration reactions in the adjacent granites and metapelites. Although texturally not preserved, these hydration reactions may have been similar (but opposite in sign) to the dehydration reactions which occurred during amphibolite facies overprinting of the country rocks enclosing the mafic eclogites (Heinrich, 1982). Because of the quantitative predominance of the pelitic, quartzofeldspathic and granitic country rocks relative to the mafics, the amount of fluid produced by high-pressure dehydration of the mafic rocks is unlikely to have been sufficient to saturate the country rock assemblages and to cause regionally extensive fluid presence during eclogite facies metamorphism. As a consequence, the net loss of volatiles during high-pressure metamorphism from the Adula Nappe as a whole was probably at most minor.

Even in the mafic eclogites of the southern Adula Nappe, fluid-present high-pressure metamorphism was probably restricted to times when major dehydration reactions were in progress. As the important dehydration reactions are sensitive to increasing pressure, the last event causing fluid saturation in the kyanite eclogites may have occurred closer to their peak metamorphic pressure, rather than near the peak temperature reached by the same rocks later on their P-T path.

CONCLUSIONS

The zoisite/epidote- and hornblende-bearing kyanite eclogites of the southern Adula Nappe are a characteristic example of 'common' or 'type-B' eclogites (Smulikowski, 1964; Coleman *et al.*, 1965). The petrological data presented above, in conjunction with those discussed by Heinrich (1982), lead to the conclusion that type-B quartz eclogites can form *in situ* (i.e. with a metamorphic history shared by their gneissic country rocks) by prograde dehydration metamorphism from more hydrous protoliths. It should be stressed that the incompatible metamorphic pressures often recorded by mafic type-B eclogites and adjacent plagioclase-rich amphibolite-facies gneisses do not provide unequivocal evidence against a common regional high-pressure metamorphic history shared by the two rock types (Heinrich, 1982).

Prograde dehydration of mafic rocks to quartz-kyanite eclogite is confined to depths below the normal continental Moho, and requires subduction or tectonic crustal thickening. Field data suggest that the transition near 12–15 kb/500–600 °C from eclogite rich in paragonite + epidote + amphibole to quartz-kyanite eclogite according to reaction (12) represents an important dehydration step in progressive high-pressure metamorphism of mafic rocks. However, even at considerably higher P–T conditions up to at least 20 kb/800 °C, minor zoisite, hornblende and phengite persist as stable hydrosilicates in quartz-kyanite eclogites of suitable bulk composition.

Near 12 kb/500 °C or less, garnet, omphacite and quartz can coexist stably with all minerals typical of albite-epidote amphibolites, but the assemblage albite + epidote + hornblende + quartz + omphacite (+ garnet) requires fluid-absent metamorphism or dilution of any hydrous fluid by other components. Rather than omphacite-garnet amphibolite, the association of omphacite + quartz (+ garnet, amphibole, epidote) with paragonite is the most likely 'eclogitic' assemblage to form by prograde dehydration metamorphism at crustal pressures of less than 10 kb.

ACKNOWLEDGEMENTS

This research was carried out as part of a Ph.D. project at ETH Zürich. I have greatly benefited from working with V. Trommsdorff and A. B. Thompson who supervised the project, contributing enthusiasm and ideas at all stages of the work through to the completion of this manuscript. The petrographic and analytical work relied on the excellent sample preparation by A. Willi, and the help of J. Sommerauer and S. Girsperger with the use of microprobe and computer facilities. I enjoyed many stimulating discussions with P. O. Koons, and with other colleagues at ETH and other Swiss universities. A. S. Andrew, M. Frey, B. Hensen, P. O. Koons and D. J. Whitford read the manuscript at various stages, and their comments were very helpful to improve its content and presentation. Reviews by W. V. Maresch and T. J. B. Holland are gratefully acknowledged. A great effort was provided by the typing office at CSIRO, Institute of Energy and Earth Resources in Sydney, where this paper was completed. To all of these people, I would like to express my thanks for their help and interest! Financial support by the Schweizerischer Nationalfonds (Project 2.805-0.80) is acknowledged.

REFERENCES

Anderson, R. N., De Long, S. F., & Schwarz, W. M., 1978. Geophysical and geochemical constraints at converging plate boundaries. *J. Geol.* **86**, 731–9.

Aurisicchio, C., Bocchio, R., Liborio, G., & Mottana, A., 1982. Petrogenesis of the eclogites from Soazza, Switzerland. *Abstr. 1st Int. Eclogite Conference, Terra cognita*, **2**, 305.

Banno, S., & Matsui, Y., 1965. Eclogite types and partition of Mg, Fe, and Mn between clinopyroxene and garnet. *Proc. Japan. Acad.* **41**, 716–21.

Baumgartner, L., 1981. Petrologie der Alp de Confin, Misox GR. *Unpublished Diploma thesis, University of Basel.*

——& Löw, S., 1983. Deformation und Metamorphose der Adula-Decke südwestlich San Bernardino, Schweiz. *Schweiz. miner. petrogr. Mitt.* **63**, 215–32.

Bearth, P., 1959. Ueber Eklogite, Glaukophanschiefer und metamorphe Pillowlaven. *Ibid.* **39**, 267–86.

Black, P. M., 1977. Regional high-pressure metamorphism in New Caledonia: phase equilibria in the Ouegoa District. *Tectonophysics*, **43**, 89–107.

Brown, E. H., & Bradshaw, J. Y., 1979. Phase relations of pyroxene and amphibole in greenstone, blueschist and eclogite of the Franciscan Complex, California. *Contr. Miner. Petrol.* **71**, 67–83.

Buletti, M., 1983. Zur Geochemie und Entstehungsgeschichte der Granat-Amphibolite des Grambarognogebietes, Ticino. *Schweiz. miner. petrogr. Mitt.* **63**, 233–47.

Carpenter, M. A., 1980. Mechanisms of exsolution in sodic pyroxene. *Contr. Miner. Petrol.* **71**, 289–300.

Chatterjee, N. D., 1972. The upper stability limit of the assemblage paragonite + quartz and its natural occurrences. *Ibid.* **34**, 288–303.

——& Johannes, W. S., 1974. Thermal stability and standard thermodynamic properties of synthetic 2M1-muscovite, $KAl_3Si_3O_{10}(OH)_2$. *Ibid.* **48**, 89–114.

Clark, J R., & Papike, J. J., 1968. Crystal-chemical characterization of omphacites. *Am Miner.* **53,** 840-68.
Codoni, A. G , 1981. Geologia e petrografia del Pizzo di Claro *PhD thesis, Zürich University.*
Coleman, R. G., Lee, D. E., Beatty, L. B., & Brannock, W. W., 1965. Eclogites and eclogites: their differences and similarities. *Bull. Geol. Soc. Am* **76,** 483-508.
Delany, J. M., & Helgeson, H. C., 1978 Calculation of the thermodynamic consequences of dehydration in subducting oceanic crust to 100 kb and > 800 °C *Am. J. Sci.* **278,** 638-86.
Egli, W., 1966. Geologisch-petrographische Untersuchungen in der NW-Aduladecke und in der Sojaschuppe (Bleniotal, Kanton Tessin). *PhD thesis, ETH Zürich.*
Ellis, D. J., & Green, D. H., 1979. An experimental study of the effect of Ca upon garnet-clinopyroxene Fe-Mg exchange equilibria. *Contr Miner. Petrol.* **71,** 13-22.
England, P. C., & Thompson, A. B., 1984. Pressure-temperature-time paths of regional metamorphism I Heat transfer during the evolution of regions of thickened continental crust. *J Petrology,* **25,** 894-928.
Ernst, W. G., 1977. Mineralogic study of eclogitic rocks from Alpe Arami, Lepontine Alps, Southern Switzerland *Ibid.* **18,** 371-98.
——1978. Petrochemical study of lherzolitic rocks from the Western Alps. *Ibid* **19,** 341-92.
——& Dal Piaz, G. V., 1978. Mineral parageneses of eclogitic rocks and related mafic schists of the Piemonte ophiolite nappe, Breuil-St. Jacques area, Italian Western Alps. *Am. Miner.* **63,** 621-40.
Essene, E. S., & Fyfe, W. S., 1967. Omphacite in Californian metamorphic rocks. *Contr. Miner. Petrol.* **15,** 1-23.
Evans, B. W., & Trommsdorff, V., 1978. Petrogenesis of garnet lherzolite, Cima di Gagnone, Lepontine Alps. *Earth planet. Sci. Lett.* **40,** 333-48
——————& Goles, G., 1981. Geochemistry of high-grade eclogites and metarodingites from the Central Alps. *Contr. Miner. Petrol.* **76,** 301-11.
——————& Richter, W., 1979. Petrology of an eclogite-metarodingite suite at Cima di Gagnone, Ticino, Switzerland. *Am. Miner.* **64,** 15-31.
Frey, M., Jäger, E., & Niggli, E., 1976. Gesteinsmetamorphose im Bereich der Geotraverse Basel-Chiasso. *Schweiz. miner. petrogr. Mitt.* **56,** 649-59.
Fry, N., & Fyfe, W. S., 1969. Eclogites and water pressure. *Contr. Miner. Petrol.* **24,** 1-6.
Gansser, A., 1937. Der Nordrand der Tambodecke. *Schweiz. miner. petrogr. Mitt.* **17,** 291-523.
Gasparik, T., & Lindsley, D. H., 1980. Phase equilibria at high pressures of pyroxenes containing monovalent and trivalent ions. In: Prewitt, C. T. (ed.) *Pyroxenes. MSA Rev. Mineralogy,* **7,** 309-39.
Green, D. H., & Ringwood, A. E., 1968. Genesis of the calc-alkaline igneous rock suite *Contr. Miner Petrol* **18,** 105-62.
Green, T. H., & Hellman, P. L., 1982. Fe-Mg partitioning between coexisting garnet and phengite at high pressure, and comments on a garnet-phengite geothermometer. *Lithos,* **15,** 253-66.
Greenwood, H. J., 1967. The N-dimensional tie-line problem. *Geochim. cosmochim. Acta,* **31,** 465-90.
——1975. Thermodynamically valid projections of extensive phase relationships. *Am. Miner.* **60,** 1-8.
Griffin, W. L., Austrheim, A., Bråstad, K., Bryhni, I., Krill, A., Krogh, E., Mørk, M. B. E., Qvale, H., & Torudbakken, B., 1985. High-pressure metamorphism in the Scandinavian Caledonides. In: Gee, D. G., & Sturt, B. A. (eds.) *The Caledonian Orogen, Scandinavia and Related Areas.* Wiley, in press.
Hänny, R., Grauert, B., & Soptrajanova, G., 1975. Paleozoic migmatites affected by high-grade Tertiary metamorphism in the Central Alps (Valle Bodengo, Italy). *Contr. Miner. Petrol.* **51,** 173-96.
Harley, S. L., & Green, D. H., 1982. Garnet-orthopyroxene barometry for granulites and peridotites. *Nature,* **300,** 697-701.
Heinrich, C. A., 1982. Kyanite-eclogite to amphibolite facies evolution of hydrous mafic and pelitic rocks, Adula Nappe, Central Alps. *Contr. Miner. Petrol.* **81,** 30-8.
——1983. Die regionale Hochdruckmetamorphose der Adula-Decke, Zentralalpen (Schweiz). *PhD thesis 7282, ETH Zürich.*
Helgeson, H. C., Delany, J. M., Nesbitt, H. W., & Bird, D. C., 1978. Summary and critique of the thermodynamic properties of rock forming minerals. *Am. J. Sci.* **278A,** 1-229.
Holdaway, M. J., 1971. Stability of andalusite and the aluminum silicate phase diagram. *Ibid.* **271,** 97-131.
Holland, T. J. B., 1979*a*. High water activities in the generation of high pressure kyanite eclogites of the Tauern Window, Austria. *J. Geol.* **87,** 1-27.
——1979*b*. Experimental determination of the reaction paragonite = jadeite + kyanite + H_2O, and internally consistent thermodynamic data for part of the system Na_2O-Al_2O_3-SiO_2-H_2O, with applications to eclogites and blueschists. *Contr. Miner. Petrol.* **68,** 293-301.
——1983. The experimental determination of activities in disordered and short-range ordered jadeitic pyroxenes. *Ibid.* **82,** 214-20.
——& Richardson, S. W., 1979. Amphibole zonation in metabasites as a guide to the evolution of metamorphic conditions. *Ibid.* **70,** 143-8.
Jenny, H., Frischknecht, G., & Kopp, J., 1923. Geologie der Adula. *Beitr. Geol. Karte Schweiz* N.F. **51.**
Koons, P. O., 1982*a*. An experimental investigation of the behaviour of amphibole in the system Na_2O-MgO-Al_2O_3-SiO_2-H_2O at high pressures. *Contr. Miner. Petrol.* **79,** 258-67.
——1982*b*. An investigation of experimental and natural high-pressure assemblages from the Sesia Zone, Western Alps. *PhD thesis 7169, ETH Zürich.*

—— 1984. Implications to garnet–clinopyroxene geothermometry of non-ideal solid solution in jadeitic pyroxenes. *Contr. Miner Petrol.* **88,** 340–7.
Krogh, E. J., 1977. Evidence of Precambrian continent–continent collision in Western Norway. *Nature,* **267,** 17–19.
—— & Raheim, A., 1978. Temperature and pressure dependence of Fe–Mg-partitioning between garnet and phengite, with particular reference to eclogites. *Contr. Miner. Petrol.* **66,** 75–80.
Laird, J., 1980 Phase equilibria in mafic schist from Vermont. *J. Petrology,* **21,** 1–37.
—— & Albee, A. L., 1981. Pressure, temperature and time indicators in mafic schist: their application to reconstructing the polymetamorphic history of Vermont. *Am. J. Sci.* **281,** 127–75.
Lambert, I. B., & Wyllie, P. H., 1972. Melting of gabbro (quartz eclogite) with excess water to 35 kilobars, with geological applications. *J. Geol* **80,** 693–708.
Leake, B. E., 1978. Nomenclature of amphiboles. *Am. Miner.* **63,** 1023–52.
Lovering, J. F., & White, A. J. R., 1969. Granulitic and eclogitic inclusions from basic pipes at Delegate, Australia. *Contr. Miner. Petrol.* **21,** 9–52.
Maresch, W., 1983. Die Bildung von Eklogit aus Amphibolit bei progressiver Hochdruckmetamorphose. *Fortschr. Miner.* **60,** Beih. **1,** 137–8.
Miyashiro, A., 1973. *Metamorphism and Metamorphic Belts.* London: Allen & Unwin.
Newton, R. C., & Fyfe, W S., 1976. High pressure metamorphism. In: Bailey, D K., & Macdonald, R. (eds.) *The Evolution of the Crystalline Rocks,* 101–86.
Oberhänsli, R., 1978 Chemische Untersuchungen an Glaukophan-führenden basischen Gesteinen aus den Bündnerschiefern Graubündens. *Schweiz. miner. petrogr. Mitt.* **56,** 139–56.
Plas, L. van der, 1959. Petrology of the northern Adula region, Switzerland. *Leidse Geol. Meded.* **24,** 415–602.
Robie, R. A., Hemingway, B. S., & Fisher, J. R., 1979. Thermodynamic properties of minerals and related substances at 298·15 K and 1 bar (105 pascals) pressure and at high temperatures. *Bull. U.S. geol. Surv.* **1452.**
Rubie, D. C., 1984. A thermal-tectonic model for high-pressure metamorphism and deformation in the Sesia Zone, Western Alps. *J. Geol* **92,** 21–36.
Smulikowski, K., 1964. An attempt at eclogite classification *Bull. Acad. Polon. Sci. (Sect. Sci. geol. geogr.)* **12,** 27–33.
Spear, F. S., 1981. Amphibole–plagioclase phase equilibria: an empirical model for the relation albite + tremolite = edenite + quartz. *Contr. Miner. Petrol.* **77,** 355–64.
Takasu, A., 1984. Prograde and retrograde eclogites in the Sambagawa metamorphic belt, Besshi District, Japan. *J Petrology,* **25,** 619–43.
Thompson, A. B., 1983. Fluid-absent metamorphism *J. geol. Soc. Lond.* **140,** 533–47
—— & Tracy, R. J., 1979. Model systems for anatexis of pelitic rocks. II. Facies series melting and reactions in the system CaO–$KAlO_2$–$NaAlO_2$–Al_2O_3–SiO_2–H_2O. *Contr. Miner. Petrol.* **70,** 429–38.
Thompson, J. B., 1955. The thermodynamic basis for the mineral facies concept. *Am. J. Sci.* **253,** 65–103.
—— 1981. An introduction to the mineralogy and petrology of the biopyriboles. In: Veblen, D. R. (ed.) *Amphiboles and other hydrous pyriboles—mineralogy. MSA Rev. Mineralogy,* **9A,** 141–88.
—— Laird, J., & Thompson, A. B., 1982. Reactions in amphibolite, greenschist and blueschist. *J. Petrology,* **23,** 1–27.
Walther, J. V., & Orville, P M , 1982. Volatile production and transport in regional metamorphism. *Contr. Miner. Petrol.* **79,** 252–7
Winkler, H. G. F., 1974. *Petrogenesis of Metamorphic Rocks.* Springer, 4th ed
Wyllie, P. J., 1971. *The Dynamic Earth.* New York: Wiley.
Zen, E-An, 1966 Construction of pressure–temperature diagrams for multicomponent systems after the method of Schreinemakers—a geometric approach. *Bull. U.S. geol. Surv.* **1225,** 1–56.

APPENDIX 1

Sampling locations (referring to Swiss coordinates) and some petrographic details of the rocks studied by microprobe (cf. Table 1, text). All samples are stored at ETH Zürich, including some collected by W. Richter, V. Trommsdorff and R. Oberhänsli.

Vals

Ad42-9-14 (734700/159000) Banded omp–gar amphibolite from Peil, earlier described by Plas (1959, p. 502). Interlocked hbl + alb poikiloblasts, other minerals form fine-grained matrix and inclusions in hbl and alb. Apparently stable coexistence of omp + alb + qtz.

VA30 (same locality) Layer of fine-grained granoblastic to schistose hydrosilicate-rich eclogite in amphibolite Ad42-9-14; mineral compositions almost identical to Ad42-9-14.

Ad41-9-20 (735500/160400) cm-thick, probably tuffaceous, layer in calc-mica schist from Mesozoic cover of Adula Nappe.

Ad65-0-8 (732750/161300) Garnet glaucophanite with Fe-rich epi and acmitic omp. Equigranular schistose texture.

Confin

Ad48-9-5 (731900/147000) Equigranular matrix with linear fabric, enclosing small euhedral gar porphyroblasts.

E5-10 (same locality) Same texture. Barroisite + kya enriched in 2 cm boudin grading into surrounding par-rich eclogite.

E5-6 (same locality) Similar texture except poikiloblastic hbl with 'myrmekitic' qtz precipitates. Hbl composition probably not primary.

Ad51-9-12 (732500/146700) Calcic eclogite rich in apparently coexisting zoi + clz. At contact of tremolite-antigorite schist—possibly metarodingite.

Ad51-9-17 (732500/146700) Dolomite marble of unknown age at serpentinite contact. Poikiloblasts of jadeite-poor omp + primary act + zoi. Partial later overprinting of zoi + dol to chlorite + clc.

Trescolmen

Ad25-9-3 (733690/139810) Granoblastic matrix with 1-5 mm kya and hbl poikiloblasts. Omp-kya-qtz veins in same outcrop.

Ad61-9-1 (733460/139690; block) Nematoblastic very qtz-rich eclogite with nearly Ca-free Mg-glaucophane. Talc later, possibly pseudomorphing earlier carbonate (cf. Holland, 1979*a*, p. 14).

Gagnone

CH271 (707960/130750) Texture as Ad25-9-3. Omp-kya-qtz veins occur in same lens.

Mg163K (708360/131060) Banded granoblastic matrix with gar as euhedral porphyroblasts and atoll-crystals. Contact of chlorite-enstatite metaperidotite (see Evans *et al.*, 1979; including analyses).

Mg163-4-8 (same locality) Equigranular layer rich in hbl + zoi, with strong grain alignment shared by omp and hydrosilicates.

E2-2 (708090/130860) Partly overprinted eclogite with porpyroblastic garnet. Clz and zoi show no reaction relationship. Some hbl secondary.

Arami

Mg9-5-12c (719000/121000) Equigranular eclogite from mafic envelope of garnet lherzolite lens. Weak schistosity defined by omp and zoi. All minerals including gar strikingly homogeneous. Hbl in matrix and as gar-inclusions, with same composition.